Rb and p130 control cell cycle gene silencing to maintain the postmitotic phenotype in cardiac myocytes

Patima Sdek,[1] Peng Zhao,[1] Yaping Wang,[1] Chang-jiang Huang,[2] Christopher Y. Ko,[1] Peter C. Butler,[2] James N. Weiss,[1] and W. Robb MacLellan[1]

[1]Cardiovascular Research Laboratory, Department of Medicine and Department of Physiology, and [2]Larry Hillblom Islet Research Center, David Geffen School of Medicine, University of California, Los Angeles, Los Angeles, CA 90095

The mammalian heart loses its regenerative potential soon after birth. Adult cardiac myocytes (ACMs) permanently exit the cell cycle, and E2F-dependent genes are stably silenced, although the underlying mechanism is unclear. Heterochromatin, which silences genes in many biological contexts, accumulates with cardiac differentiation. H3K9me3, a histone methylation characteristic of heterochromatin, also increases in ACMs and at E2F-dependent promoters. We hypothesize that genes relevant for cardiac proliferation are targeted to heterochromatin by retinoblastoma (Rb) family members interacting with E2F transcription factors and recruiting heterochromatin protein 1 (HP1) proteins. To test this hypothesis, we created cardiac-specific Rb and p130 inducible double knockout (IDKO) mice. IDKO ACMs showed a decrease in total heterochromatin, and cell cycle genes were derepressed, leading to proliferation of ACMs. Although Rb/p130 deficiency had no effect on total H3K9me3 levels, recruitment of HP1-γ to promoters was lost. Depleting HP1-γ up-regulated proliferation-promoting genes in ACMs. Thus, Rb and p130 have overlapping roles in maintaining the postmitotic state of ACMs through their interaction with HP1-γ to direct heterochromatin formation and silencing of proliferation-promoting genes.

Introduction

Some amphibians, as well as teleost fish, have a robust capacity to regenerate their hearts after injury throughout their life (Poss et al., 2002). Adult zebrafish, for example, can fully regenerate their heart without scar formation after up to 20% of the ventricle has been resected. This regenerative response is thought to occur primarily through dedifferentiation and proliferation of existing myocytes (Jopling et al., 2010; Kikuchi et al., 2010). Recent studies have demonstrated that the embryonic mammalian heart is also capable of mounting a hyperplastic response to injury but that this is lost rapidly after birth (Drenckhahn et al., 2008; Porrello et al., 2011). Although some studies have suggested that the adult mammalian heart possesses a very limited capacity for new cardiomyocyte formation, the source has been postulated to be endogenous cardiac stem cells, not existing myocytes (Pasumarthi and Field, 2002; Hsieh et al., 2007; Bergmann et al., 2009). Thus, the vast majority of cardiac myocytes permanently exits the cell cycle soon after birth in mammals, and, when adult cardiac myocytes (ACMs) are subjected to a growth stimulus, they undergo an increase in cell size (hypertrophy) but do not proliferate. The molecular basis for the postmitotic state of ACMs is unknown, but the subset of E2F-dependent genes specifically involved in regulating G2/M and cytokinesis is not up-regulated after growth stimuli in ACMs. The mechanisms that irreversibly silence these genes are unknown; however, stable transcriptional silencing in eukaryotic cells is often caused by specific histone modifications that result in heterochromatin formation around a gene, making it inaccessible to transcriptional machinery.

Correspondence to W. Robb MacLellan: rmaclellan@mednet.ucla.edu

Abbreviations used in this paper: ACM, adult cardiac myocyte; ANF, atrial natriuretic factor; ChIP, chromatin IP; HP1, heterochromatin protein 1; IDKO, inducible double knockout; IP, immunoprecipitation; ITS, insulin-transferrin-selenium; MCM, MerCreMer; MHC, myosin heavy chain; NI, nonionic; NRVM, neonatal rat ventricular myocyte; NS, nonspecific; PSG, penicillin-streptomycin-glutamine; Rb, retinoblastoma; TAC, trans-aortic constriction; TAM, tamoxifen; TLVM, time-lapse video microscopy; WT, wild type.

The Rockefeller University Press $30.00
J. Cell Biol. Vol. 194 No. 3 407–423
www.jcb.org/cgi/doi/10.1083/jcb.201012049

Chromatin is remodeled into active (euchromatin) and silent (heterochromatin) regions through covalent modification of DNA and histones. These modifications regulate chromatin structure and gene expression. Histone acetylation, established by histone acetyltransferases, generally correlates with gene activation and is essential for animal development. Two distinct families of histone acetyltransferases, GCN5 and PCAF (P300/CBP-associated factor; acetyltransferases of H3K9) and CBP and p300 (acetyltransferases of H3K18/27), have been demonstrated to be involved in E2F-dependent gene expression, and the deletion of either of them in mice leads to early embryonic lethality (Lang et al., 2001; Roth et al., 2001; Wang et al., 2007; Jin et al., 2011). The role of histone acetylation in cardiac myocytes has received much attention as a means of promoting euchromatin (Shogren-Knaak et al., 2006) and activating gene expression in the heart (Haberland et al., 2009). In contrast, the role of histone methylation in cardiac growth has been largely ignored despite its critical role in regulating gene expression in many cell types. Both the position and the degree of methylation may either activate or silence gene expression (Martin and Zhang, 2005; Shi, 2007). In animals, both H3K9me2 and H3K9me3 are related to gene silencing (Krauss, 2008); however, H3K9me3 is found predominantly within heterochromatin, whereas H3K9me2 is mostly associated with silent domains within the euchromatic regions (Peters et al., 2001; Lehnertz et al., 2003). H3K9me1 and H3K9me2 are catalyzed by the histone methyltransferase G9a, whereas H3K9me3 is established by the histone methyltransferase Suv39h1 (Brenner and Fuks, 2007; Chin et al., 2007), which is often expressed in senescence and postmitotic cells (Rice et al., 2003). Trimethylation of lysine 27 on histone H3 (H3K27me3) has also been associated with heterochromatin formation and transcriptional repression (Dillon, 2004). The establishment of H3K27me3 is a result of the methyltransferase activity of polycomb group multiprotein complexes PRC1 or PRC2. Ezh2, the catalytic subunit of PRC2, had been thought to be the sole H3K27 methyltransferase (Schuettengruber et al., 2007). Recently, however, Ezh1 was also shown to have H3K27 methyltransferase activity (Shen et al., 2008). Ezh1 and Ezh2 form similar PRC2 complexes but exhibit contrasting repressive roles (Margueron et al., 2008). Ezh2 expression is associated with proliferation, whereas Ezh1 is typically more abundant in nonproliferative adult organs (Laible et al., 1997).

One of the primary mechanisms by which histone modifications transmit their biological signals is through binding of effector proteins that recognize distinct modifications (Fischle et al., 2003a; Daniel et al., 2005). H3K9me3 and H3K27me3 are preferentially recognized by the chromodomain-containing proteins heterochromatin protein 1 (HP1; Lachner et al., 2001) or Pc2 (Fischle et al., 2003b; Min et al., 2003), respectively. HP1 is a family of proteins (α, β, and γ) that plays an important role in gene silencing in many organisms (James and Elgin, 1986; Kellum, 2003) by establishing and maintaining heterochromatin (Daniel et al., 2005), but their role in the heart is unknown. HP1 family members typically differ in their subcellular localization and interaction partners and thus likely have distinct cellular functions (Minc et al., 1999, 2001; Auth et al., 2006). The structure of Pc2 bound to H3K27me3 is very similar to that of HP1-binding H3K9me3. Functionally, the Pc2-containing PRC1 complex stabilizes the repression of chromatin structure by antagonizing the switch–sucrose nonfermentable complex (Shao et al., 1999).

The mechanisms whereby distinct histone modifications or chromatin is localized to specific genes are an area of intense research. Retinoblastoma (Rb) family members can direct H3K9me3 and H3K27me3 to specific promoter regions, providing a means to target cell cycle genes to heterochromatin through their ability to interact with E2F family members and recruit repressive chromatin remodeling factors to E2F-dependent promoters (Nielsen et al., 2001; Blais et al., 2007). Rb can potentially associate with multiple chromatin remodeling factors, including histone deacetylases (Luo et al., 1998; Magnaghi-Jaulin et al., 1998), Suv39h1 (Nielsen et al., 2001), HP1 (Nielsen et al., 2001), and Pc2 (Dahiya et al., 2001). In senescent cells, Rb promotes heterochromatin formation at E2F-responsive genes by recruiting HP1 to H3K9 trimethylated promoters, thereby producing a permanent insensitivity to mitogenic signals (Nielsen et al., 2001; Narita et al., 2003). Pc2 has also been implicated in the repression of the E2F-dependent genes and can cooperate with Rb to inhibit the expression of cyclin A and cdc2 (Dahiya et al., 2001).

Despite numerous descriptive studies (Soonpaa and Field, 1994; Li et al., 1996; Bergmann et al., 2009; Walsh et al., 2010) characterizing the limited ability of ACMs to proliferate, almost no mechanistic data exist to explain why ACMs do not reenter the cell cycle in response to mitogenic stimuli. We have implicated Rb family members in mediating cardiac cell cycle exit (MacLellan et al., 2005), but what role they play in maintaining the postmitotic state of ACMs and the mechanisms underlying their importance are unknown. Indeed, recent studies have questioned whether Rb family members actually play any role in the maintenance of terminal differentiation (Camarda et al., 2004; Huh et al., 2004; Mantela et al., 2005; Blais et al., 2007). Here, we demonstrate that heterochromatin accumulation and targeting of proliferation-promoting genes to these transcriptionally silent regions are the molecular basis of the postmitotic phenotype of ACMs. Rb and p130 target E2F-dependent genes to heterochromatin in ACMs, silencing these proliferation-promoting genes through the recruitment of HP1-γ to H3K9 trimethylated promoters.

Results

Silencing of E2F-dependent genes in ACMs is associated with H3K9me3 and heterochromatin formation

To clarify the expression pattern of cell cycle genes in cardiac myocytes, we compared expression levels of cell cycle genes in purified embryonic (embryonic day 15.5 [E15.5]) cardiac myocytes, ACMs, and growth-stimulated ACMs. To provide a growth stimulus for ACMs in vivo, trans-aortic constriction (TAC) was performed, which leads to pressure overload and primarily hypertrophic growth. Embryonic cardiac myocytes expressed high levels of all cell cycle genes consistent with their proliferative

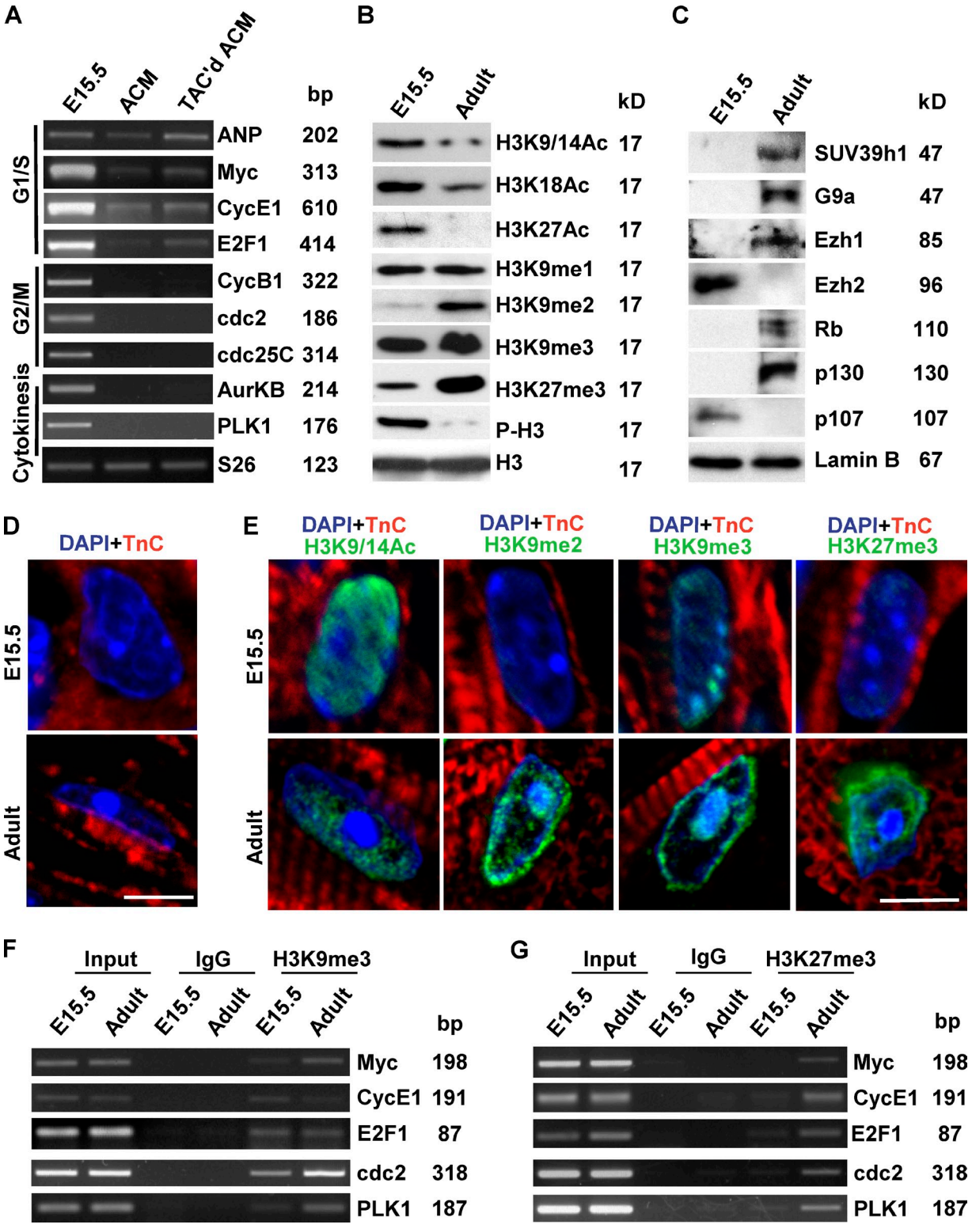

Figure 1. **Silencing of E2F-dependent genes in ACMs is associated with heterochromatin formation and H3K9 and H3K27 trimethylation.** (A) To quantify cell cycle genes in ACMs after a growth stimulus, semiquantitative RT-PCR was performed on total RNA isolated from purified primary cardiac myocytes at the indicated developmental time points or 7 d after TAC-induced pressure overload. ANP, atrial natriuretic peptide; AurKB, Aurora kinase B. (B) Western blots on nuclear extracts prepared from purified embryonic cardiac myocytes or ACMs demonstrate that histone H3 becomes hypoacetylated and accumulates H3K9me3 and H3K27me3 modifications with cardiac differentiation. (C) Suv39h1 and Ezh1, along with Rb and p130, are up-regulated in ACMs. (D and E) ACM nuclei demonstrated large, dense heterochromatin foci that have a lack of H3K9/14Ac and are enriched for H3K9me3. Confocal microscopy was performed on myocardial sections from WT C57/BL6 embryonic (E15.5) and adult mice after immunostaining (red, troponin C [TnC]; green, indicated histone H3 modification; blue, DAPI). Bars, 5 µm. (F and G) H3K9me3 (F) and H3K27me3 (G) were increased at promoters of E2F-dependent cell cycle genes after cardiac terminal differentiation. For quantitation of changes, see Fig. S1. ChIP was performed using chromatin extracts from purified myocytes and PCR for E2F-dependent promoters.

state (Fig. 1 A). Although G1/S genes (CycD1 and Myc) were up-regulated in ACMs after pressure overload in vivo, expression of the subset of cell cycle genes that regulates G2/M (CycB1, cdc2, and cdc25C) and cytokinesis (Aurora kinase B and pololike kinase 1 [PLK1]) was not detectable in ACMs and remained unchanged after TAC, whereas pressure overload in ACMs resulted in up-regulation of the ventricular hypertrophy marker atrial natriuretic peptide (also known as atrial natriuretic factor [ANF]; Fig. 1 A). We examined embryonic cardiac myocytes or ACMs for the developmental pattern of histone modifications and the expression of proteins that regulate these posttranslational modifications. H3K9me2/3 and H3K27me3, the histone modifications associated with transcription repression, are increased in ACMs, whereas histone modifications associated with active gene expression (H3K9/14Ac, H3K18Ac, and H3K27Ac) and mitosis (phosphorylation of histone H3S10) are decreased (Fig. 1 B). Consistent with these alterations, H3K9 and H3K27 methyltransferases G9a, Suv39h1, and Ezh1, along with Rb and p130, are up-regulated in ACMs (Fig. 1 C).

To determine whether heterochromatin aggregation accumulates with cardiac differentiation, we examined DNA in embryonic cardiac myocytes (E15.5) versus ACM nuclei for heterochromatin (Fig. 1 D). DNA within embryonic cardiac myocyte nuclei was homogeneously dispersed with limited DAPI-positive foci indicative of heterochromatin. In contrast, >90% of ACM nuclei demonstrated large, dense DAPI-positive heterochromatin foci. To further characterize these DNA foci, we immunostained cardiac nuclei for euchromatin (H3K9/14Ac) and heterochromatin (H3K9me3) markers (Figs. 1 E and S1 A). H3K9/14Ac was largely excluded from the dense DAPI-positive foci in ACMs, whereas H3K9me3 was concentrated in these DNA foci. H3K9me2 and H3K27me3 staining was found throughout nuclei in both euchromatic and heterochromatic regions, although the levels of these modifications increased dramatically from embryonic cardiac myocytes (E15.5) to ACMs (Fig. 1 E). To determine whether the H3K9me3 or H3K27me3 was associated with E2F-dependent promoters, isolated myocytes from embryonic or adult hearts were cross-linked, and H3K9me3- and H3K27me3-associated promoter sequences were determined by chromatin immunoprecipitation (IP [ChIP]). As shown, H3K9me3 and H3K27me3 were enriched at E2F-dependent G2/M (cdc2) and cytokinesis (PLK1) promoters in ACM compared with embryonic cardiac myocytes (Figs. 1 [F and G] and S1 [B and C]). Because H3K9 and H3K27 were also trimethylated at the promoter of Myc, which is up-regulated with hypertrophic stimuli, it suggests that, if H3K9me3 and H3K27me3 contribute to permanent gene silencing in ACMs, additional factors must be required.

Rb and p130 play an overlapping role in the establishment of heterochromatin formation in differentiating cardiac myocytes

There is well-documented redundancy in Rb family members (Lee et al., 1996), and our own data have demonstrated that defects in cardiac cell cycle control required deletion of both Rb and p130 (MacLellan et al., 2005). We used a cardiac-specific Cre/loxP system to delete Rb specifically in cardiac myocytes at a developmental time point at which they were still cycling. The α–myosin heavy chain (MHC [α-MHC])–driven Cre transgenic mouse we used excised Rb genomic sequences in the perinatal period before cardiac myocytes were fully differentiated (Marino et al., 2000; MacLellan et al., 2005). These cardiac-specific Rb-deficient mice ($CRb^{L/L}$) were bred to mice with a germline deletion of p130. Deletion of both Rb and p130 in cardiac myocytes led to marked defects in differentiation and cell cycle exit, whereas the single deletions were innocuous (MacLellan et al., 2005). To determine the role of Rb and p130 in heterochromatin formation in cardiac myocytes, we examined hearts from single or combined Rb and p130 knockout mice. We examined myocardial sections from control ($CRb^{+/+}$;$p130^{+/+}$), cardiac-specific Rb-deficient mice ($CRb^{L/L}$;$p130^{+/+}$), p130-deficient mice ($CRb^{+/+}$;$p130^{-/-}$), or double Rb;p130-deficient mice ($CRb^{L/L}$;$p130^{-/-}$; Fig. 2 A). Heterochromatin formation was disrupted specifically in $CRb^{L/L}$;$p130^{-/-}$ hearts. No abnormalities were seen in single Rb- or p130-deficient hearts (Fig. 2 A). Immunostaining of myocardial sections demonstrated typical heterochromatin aggregates in control myocyte nuclei; however, heterochromatin was absent, and H3K9me3 immunostaining was diffuse in Rb;p130-null myocyte nuclei (Fig. 2 B). H3K27me3 levels were dramatically decreased in $CRb^{L/L}$;$p130^{-/-}$ myocardium (Fig. 2 C). Although these results support the notion that Rb and p130 are required for controlling cell cycle exit in the cardiac myocyte, this mouse model cannot distinguish between a primary role for them in initiating terminal differentiation and heterochromatin formation in cardiac myocytes versus a secondary defect related to persistent expression of cell cycle proteins and a persistent immature state. Also, this model could not determine whether Rb and p130 are also required for the maintenance of terminal differentiation and heterochromatin once formed.

Creation of cardiac-specific Rb and p130 inducible double knockout (IDKO) mice

To determine the role of Rb and p130 more directly on heterochromatin and maintenance of the postmitotic state in fully differentiated ACMs, we created inducible, cardiac-specific double knockout mice. $Rb^{L/L}$;$p130^{-/-}$ mice were bred to α-MHC–MerCreMer (MCM) mice to generate MCM^{+};$Rb^{L/L}$;$p130^{-/-}$ mice, in which Rb can be selectively and efficiently deleted in ACMs after Cre is activated by tamoxifen (TAM). Adult (8 wk after birth) MCM^{-};$Rb^{L/L}$;$p130^{+/+}$, MCM^{+};$Rb^{L/L}$;$p130^{+/+}$, MCM^{-};$Rb^{L/L}$;$p130^{-/-}$, and MCM^{+};$Rb^{L/L}$;$p130^{-/-}$ littermates display normal heart weight to body weight ratio and left ventricle function before TAM treatment. There were no differences in expression of cell cycle genes or histone methylations (Fig. S2, A–C), indicating that neither p130 deletion nor expression of MCM by themselves had any epigenetic effect. Adult MCM^{-};$Rb^{L/L}$;$p130^{+/+}$, MCM^{+};$Rb^{L/L}$;$p130^{+/+}$, MCM^{-};$Rb^{L/L}$;$p130^{-/-}$, and MCM^{+};$Rb^{L/L}$;$p130^{-/-}$ littermates were fed with TAM chow for 14 d, resulting in four functional phenotypes: control, Rb-, p130-, and Rb/p130-deficient (IDKO) mice (Fig. 3, A and B). The minor amount of residual Rb expression likely represents the low level expression of Rb in nonmyocytes as well as unrecombined Rb in a minority of ACMs. Unless specifically indicated, analyses were performed 4 wk after

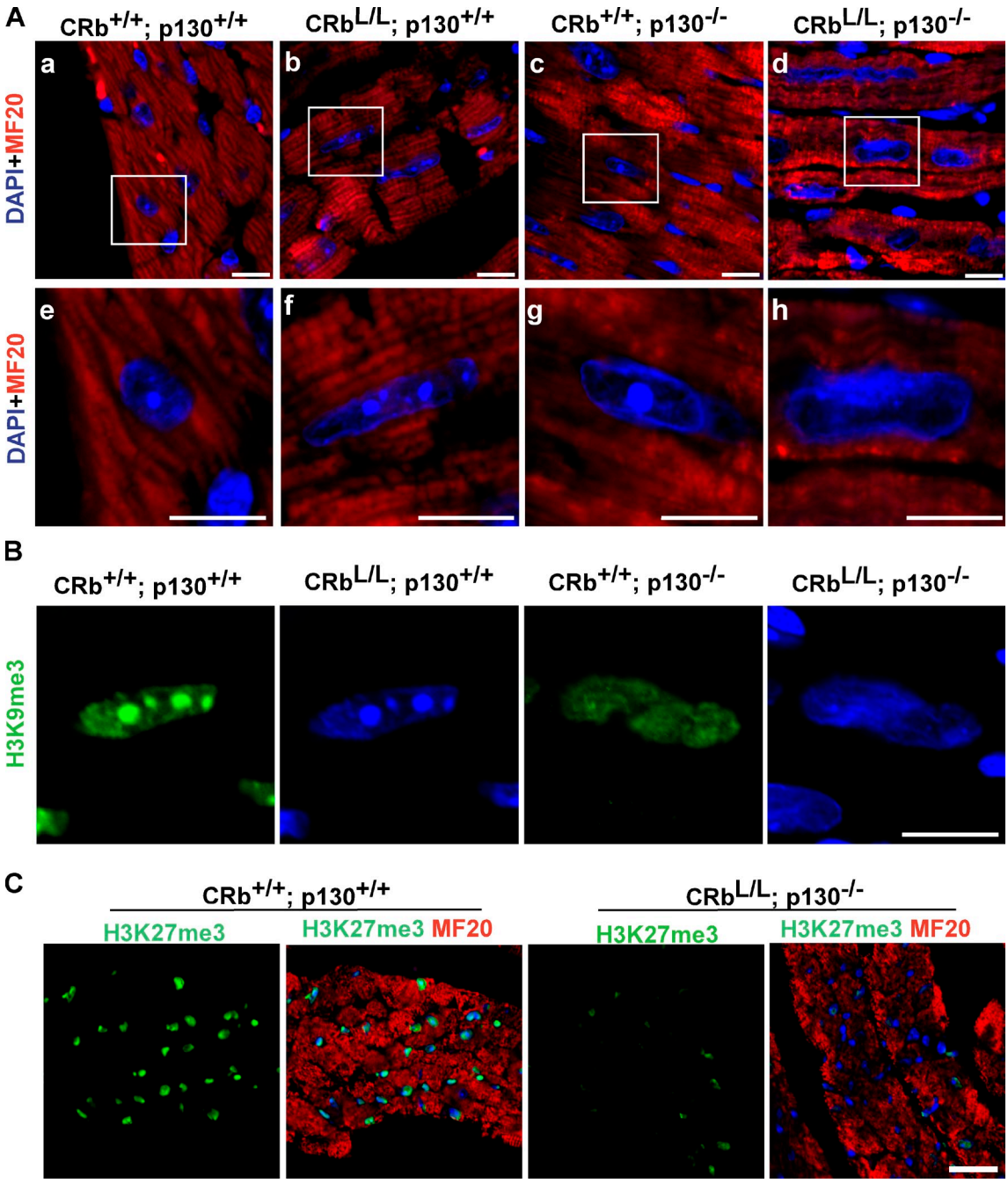

Figure 2. **Rb and p130 have overlapping roles in the establishment of heterochromatin and H3K27me3 in differentiating cardiac myocytes.** (A–C) Confocal microscopy was performed on myocardial sections from adult mice with the indicated genotypes (red, troponin C; green, indicated H3K9 or H3K27 modification; blue, DAPI). (A and B) Formation of H3K9me3-enriched heterochromatic foci was disrupted specifically in ACMs from $CRb^{L/L}$;$p130^{-/-}$ mice. Panels e–h are enlarged images of the boxed areas in panels a–d. Bars, 5 µm. (C) H3K27me3 levels were dramatically decreased in $CRb^{L/L}$;$p130^{-/-}$ myocardium compared with $CRb^{+/+}$;$p130^{+/+}$ myocardium. Bar, 25 µm.

stopping TAM to avoid any nonspecific (NS) effects related to treatment (Koitabashi et al., 2009). Fetal cardiac genes, including ANF, β-MHC, and skeletal α-actin, were up-regulated specifically in IDKO hearts, whereas the cardiac genes (such as cardiac α-actin and α-MHC) that were predominantly expressed in the ACMs remained unchanged (Fig. 3 B). IDKO ACMs reexpressed a panel of fetal cardiac-specific genes, including a 3.7-fold increase in ANF, a threefold increase of β-MHC, and a 2.3-fold increase of skeletal actin (Fig. S3 A). Histological examination of IDKO myocardium revealed large, hyperchromatic nuclei, consistent with cycling cells (Fig. 3 C). There was no increase in myocardial fibrosis or apoptosis observed in IDKO hearts (Fig. S3, B and C). Although normal at the baseline, IDKO mice developed left ventricle dilation and systolic dysfunction after TAM treatment (Table I). This contractile defect was intrinsic to the myocytes themselves, as fractional shortening of isolated IDKO ACMs was reduced (Fig. S3 D).

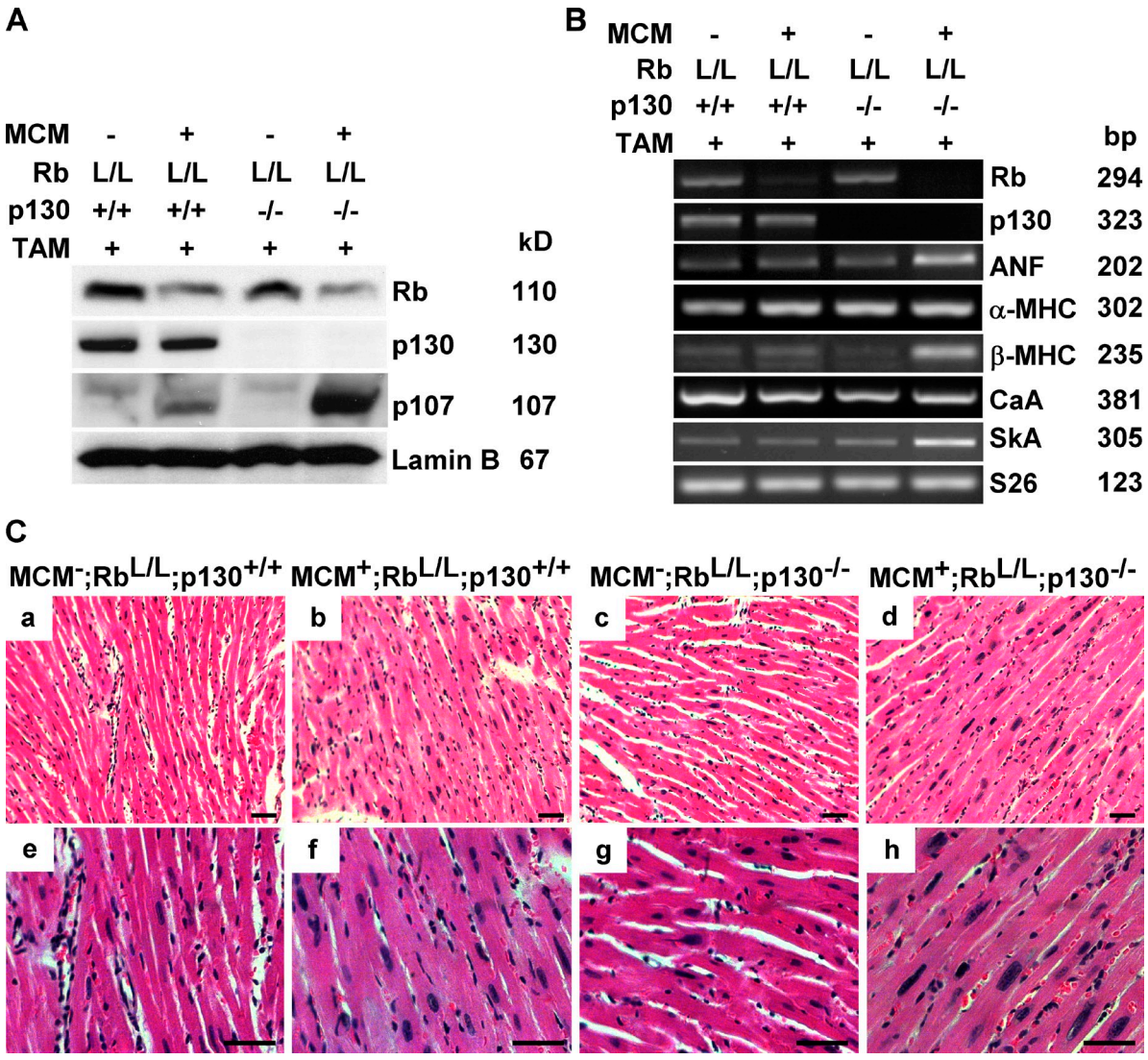

Figure 3. **Creation of IDKO mice.** (A) A Western blot using nuclear extracts prepared from ventricles of the indicated genotypes and demonstrating reductions in Rb protein levels after TAM treatment. (B) Expression of fetal cardiac-specific genes is up-regulated specifically in IDKO hearts. Semiquantitative RT-PCR was performed on total RNA extracted from purified ACMs with the indicated genotypes. For quantitation of changes in gene expression, see Fig. S3 A. CaA, cardiac actin; SkA, skeletal actin. (C) Hematoxylin and eosin staining of myocardial sections from mice with the indicated genotypes 1 wk after TAM treatment. Bars, 40 µm.

Depletion of Rb and p130 in ACMs derepresses G2/M and cytokinesis genes and disrupts heterochromatin aggregation

To determine whether Rb and p130 are involved in cell cycle gene silencing in postmitotic ACMs, expression of E2F-dependent genes was examined in IDKO mice. There was a 7–27-fold increase in expression of cell cycle genes in IDKO hearts compared with control mice, including genes involved in regulating G2/M and cytokinesis, which were stably silenced in control ACMs (Figs. 4 A and S4 A). Phosphorylation of H3S10, which is characteristic of G2/M, was also increased in IDKO hearts, but there was no change in global levels of H3K9me3 and H3K27me3 (Figs. 4 B and S4 [B and C]). Levels of H3K9me2, as well as G9a, the H3k9me2-specific methyltransferase, were decreased in ACMs from single Rb-deficient or IDKO mice, correlating with the up-regulation of G1/S cell cycle genes (cyclin E1 and E2F), which were regulated with hypertrophic stimuli. However, Rb-deficient ACMs do not reenter the cell cycle after growth stimuli, indicating that H3K9me2 is not sufficient for permanent cell cycle arrest. This reexpression of proliferation-promoting genes was associated with a marked reduction in the number of ACMs displaying heterochromatin aggregation (90 ± 1% in control ACMs vs. 14 ± 2% in IDKO ACMs, $P < 0.01$; Fig. 4, C and D). Consistent with the loss of heterochromatin, H3K9me3 immunostaining was diffuse in IDKO myocyte nuclei (Fig. S4 B). To determine whether depleting Rb and p130 also altered H3K9me3 or H3K27me3 at E2F-dependent promoters, isolated ACMs from IDKO and control hearts were cross-linked, and H3K9me3- and H3K27me3-associated promoter sequences were determined by ChIP. As shown, H3K9me3 and H3K27me3 levels at these E2F-dependent promoters remained unchanged (Fig. 4, E and F), suggesting that Rb and p130 are dispensable for maintaining these two types of histone modifications in ACMs.

Table I. **Assessment of left ventricular size and function**

Parameter	MCM$^-$;Rb$^{L/L}$;p130$^{+/+}$	MCM$^+$;Rb$^{L/L}$;p130$^{+/+}$	MCM$^-$;Rb$^{L/L}$;p130$^{-/-}$	MCM$^+$;Rb$^{L/L}$;p130$^{-/-}$
TAM	+	+	+	+
HR (bpm)	477 ± 6	473 ± 14	475 ± 16	480 ± 12
EF (%)	56.13 ± 2.02	50.40 ± 2.65	56.39 ± 3.32	33.52 ± 2.81[a]
FS (%)	28.88 ± 1.29	25.32 ± 1.59	29.13 ± 2.31	15.97 ± 1.50[a]
LVID;d (mm)	3.87 ± 0.07	3.98 ± 0.15	3.76 ± 0.02	4.78 ± 0.28[a]
LVID;s (mm)	2.74 ± 0.08	2.98 ± 0.16	2.67 ± 0.08	4.02 ± 0.28[a]
LVPW;d (mm)	0.63 ± 0.03	0.65 ± 0.14	0.67 ± 0.02	0.78 ± 0.03[a]
LVPW;s (mm)	0.89 ± 0.02	0.89 ± 0.03	0.89 ± 0.02	0.78 ± 0.03[a]

2D echocardiographic analysis of left ventricle function in mice with the indicated genotypes 4 wk after TAM treatment. *n* = 5 mice per group. Results are presented as the mean ± SEM. HR, heart rate; EF, ejection fraction; FS, fractional shortening; LVID;d/s, left ventricular internal dimension in diastole/systole; LVPW;d/s, left ventricular posterior wall thickness in diastole/systole.

[a]$P < 0.05$ by analysis of variance for MCM$^-$;Rb$^{L/L}$;p130$^{+/+}$, MCM$^+$;Rb$^{L/L}$;p130$^{+/+}$, and MCM$^-$;Rb$^{L/L}$;p130$^{-/-}$ versus MCM$^+$;Rb$^{L/L}$;p130$^{-/-}$ littermates.

IDKO ACMs spontaneously proliferate

To determine the effects of depleting Rb and p130 on cardiac myocyte growth and proliferation, we examined heart size and indices of cell cycle progression. When we examined hearts 4 wk after completing the TAM treatment, IDKO hearts displayed a 32% increase in the heart weight to body weight ratio compared with control heart (6.01 ± 0.37 vs. 4.55 ± 0.11 mg/g, $P < 0.05$; Fig. 5 A), which was directly attributable to an increase in heart weight (Fig. S5 B). To determine whether this increase in heart size was related to hypertrophy or proliferation of ACMs, we measured the cell size of isolated ACMs from control versus IDKO hearts. IDKO ACMs displayed a typical rod-shaped morphology but were 5% smaller than control ACMs (Figs. 5 B and S5 [A, C, and D]), suggesting that the increased heart size must be related to ACM proliferation. To confirm that ACMs in IDKO hearts were cycling, we determined S phase nuclei at the baseline or after hemodynamic stress. ACMs in the sham (a control surgical procedure similar to TAC)-operated IDKO myocardium demonstrated a 27-fold increase in BrdU-positive myocyte nuclei compared with the control myocardium ($P < 0.001$), which increased to 70-fold after pressure overload ($P < 0.001$; Fig. 5, C and D). Notably, BrdU staining was only detected in cardiac myocytes that had lost heterochromatin foci (Fig. S5 E). We further assessed the proliferation potential of isolated IDKO ACMs by time-lapse video microscopy (TLVM; Fig. 5 E and Video 1). ACMs from control or IDKO hearts were cultured for 8 d, and cardiac myocyte nuclei were identified by infection with an adenovirus expressing a cardiac-specific histone 2B–GFP fusion protein. ACMs lose their typical rod-shaped morphology and dedifferentiate when cultured for extended periods of time (Bersell et al., 2009), but this occurred more rapidly in IDKO myocytes. After 8 d in culture, 5.4% of IDKO ACMs completed cytokinesis during the 24-h monitoring period compared with zero control ACMs ($P < 0.01$), confirming that the proliferative potential of IDKO myocytes was restored.

Rb/p130-dependent recruitment of HP1-γ to E2F-responsive promoters is essential for irreversible silencing of proliferation-promoting genes in ACMs

It has been suggested that the ability of Rb to stably repress transcription is related to its capacity to recruit HP1 to target gene promoters, resulting in their incorporation into heterochromatin (Nielsen et al., 2001; Narita et al., 2003). All three HP1 family members are expressed in ACMs, although their subnuclear localization differs (Fig. 6 A). HP1-α and HP1-β localize in both euchromatin and heterochromatin, whereas HP1-γ is restricted to heterochromatin (Fig. 6 A). To study the role of HP1 family members on irreversible cell cycle exit in postmitotic ACMs, we depleted expression of specific HP1s in primary wild-type (WT) ACMs using siRNA and then stimulated the myocytes with serum to induce cell cycle reentry. Cells transfected with NS siRNA were used as a negative control. Each siRNA was able to specifically and effectively knock down expression of the respective HP1 (Fig. 6 B); however, expression of G2/M and cytokinesis genes only increased in HP1-γ–depleted ACMs ($P < 0.05$; Fig. 6, B and C). There was no change in the expression of Myc and ANF, which are not stably silenced in ACMs. Because HP1-γ associates with the Rb protein in ACMs (Fig. 6 D), it is an excellent candidate to mediate the stable silencing of G2/M and cytokinesis genes in ACMs.

We further examined the role of HP1-γ in cardiac myocyte cell cycle regulation by determining the effects of depleting HP1-γ in neonatal rat ventricular myocytes (NRVMs). NRVMs were transfected with NS or HP1-γ siRNA. After 48 h, cells were collected for Western blot analysis (Fig. 6 E) or stimulated with serum in the presence of BrdU (Fig. 6 F). Western blotting demonstrated efficient and specific HP1-γ knockdown. S phase myocyte nuclei were increased in HP1-γ siRNA–transfected cells compared with those transfected with NS siRNA (10.11 ± 1.79 vs. 2.34 ± 0.42%, $P < 0.001$; Fig. 6 G). To determine whether DNA synthesis is followed by cytokinesis in these myocytes, we also quantified total cell number after serum stimulation. Depletion of HP1-γ resulted in a 56% increase in the NRVM cell number ($P < 0.05$; Fig. 6 H).

HP1 recruitment to genomic sites classically occurs by binding to H3K9me3 at specific target genes (Bannister et al., 2001). However, HP1-γ also interacts with Rb, and H3K9me3 was not altered at G2/M and cytokinesis gene promoters in IDKO ACMs (Fig. 4 E). Thus, we examined whether depleting Rb and p130 might prevent recruitment of HP1-γ, despite the presence of H3K9me3. ChIP for HP1-γ was performed on isolated control and IDKO ACMs. HP1-γ was bound to cdc2 and

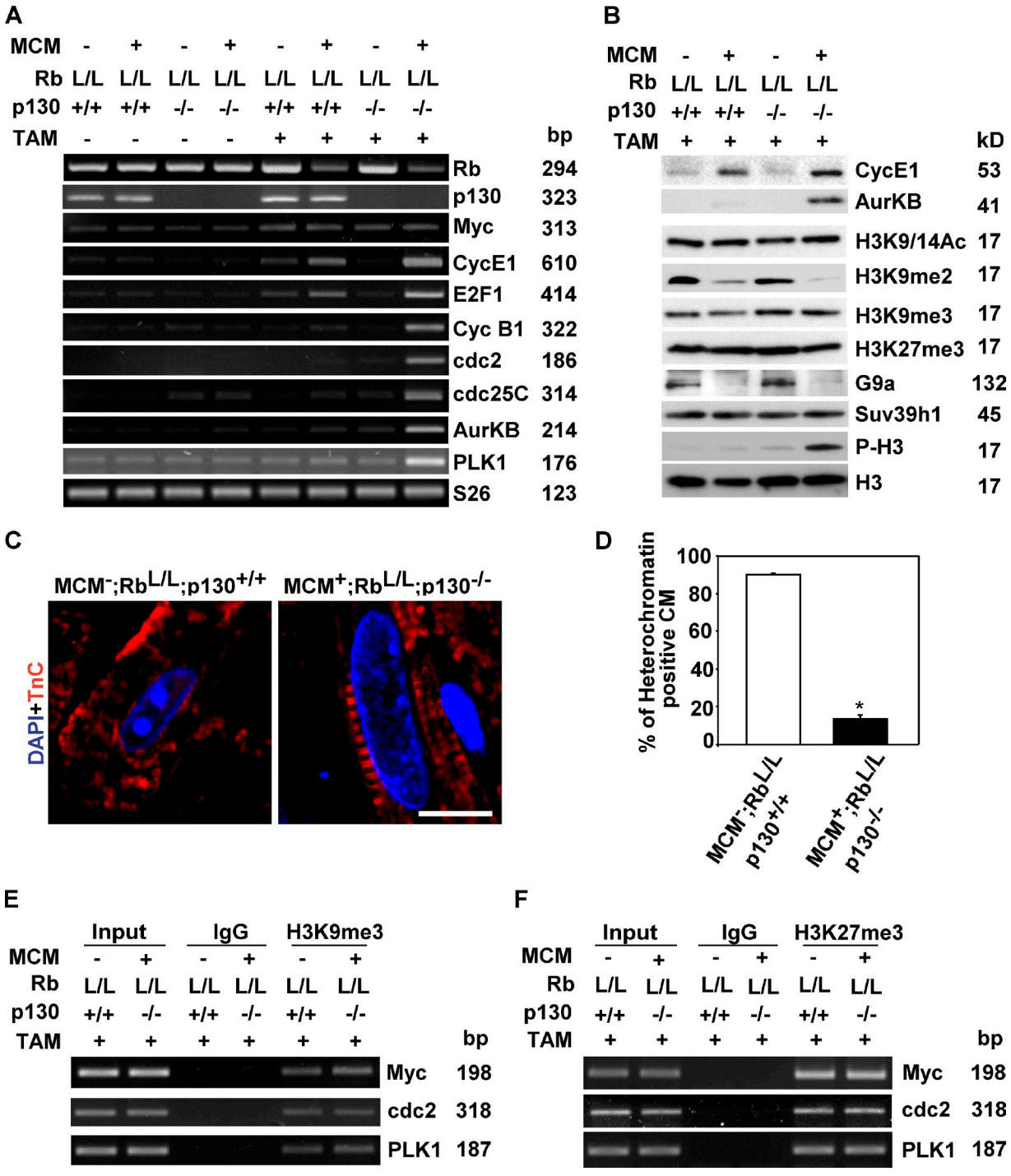

Figure 4. **Rb and p130 play an overlapping role in the silencing of proliferation-promoting genes and the maintaining of heterochromatin in ACMs.** (A) Reexpression of G2/M and cytokinesis genes in IDKO hearts. Semiquantitative RT-PCR was performed on total RNA isolated from ventricular tissue from mice with the indicated genotypes. For quantitation of changes in gene expression, see Fig. S4 A. AurKB, Aurora kinase B. (B) Western blotting demonstrates that H3K9me3 and H3K27me3 levels are unchanged in IDKO ventricles. Also see Fig. S4 (B and C) for H3K9me3 and H3K27me3 levels in isolated ACMs determined by immunostaining. (C) Heterochromatin was disrupted only in ACMs from IDKO mice. Confocal microscopy was performed on myocardial sections (red, troponin C [TnC]; blue, DAPI). Bar, 10 µm. (D) Percentages of heterochromatin-positive nuclei were quantified in ACMs isolated from hearts with the indicated genotypes and treatment (n = 3 per group; *, $P < 0.0001$). Error bars represent the SEM. CM, cardiac myocyte. (E and F) H3K9me3 (E) and H3K27me3 (F) levels at E2F-dependent promoters remained unchanged in IDKO ACMs, as analyzed by ChIP using chromatin extracts from purified myocytes.

PLK1 promoters in control ACMs, but this binding was disrupted in IDKO myocytes (Fig. 7, A and B). This was not related to lower levels of the HP1-γ protein, as expression of HP1-γ was increased in IDKO ACMs compared with control ACMs (Fig. 7 C). These results indicate that the recruitment of HP1-γ to promoters of cdc2 and PLK1 is Rb and p130 dependent.

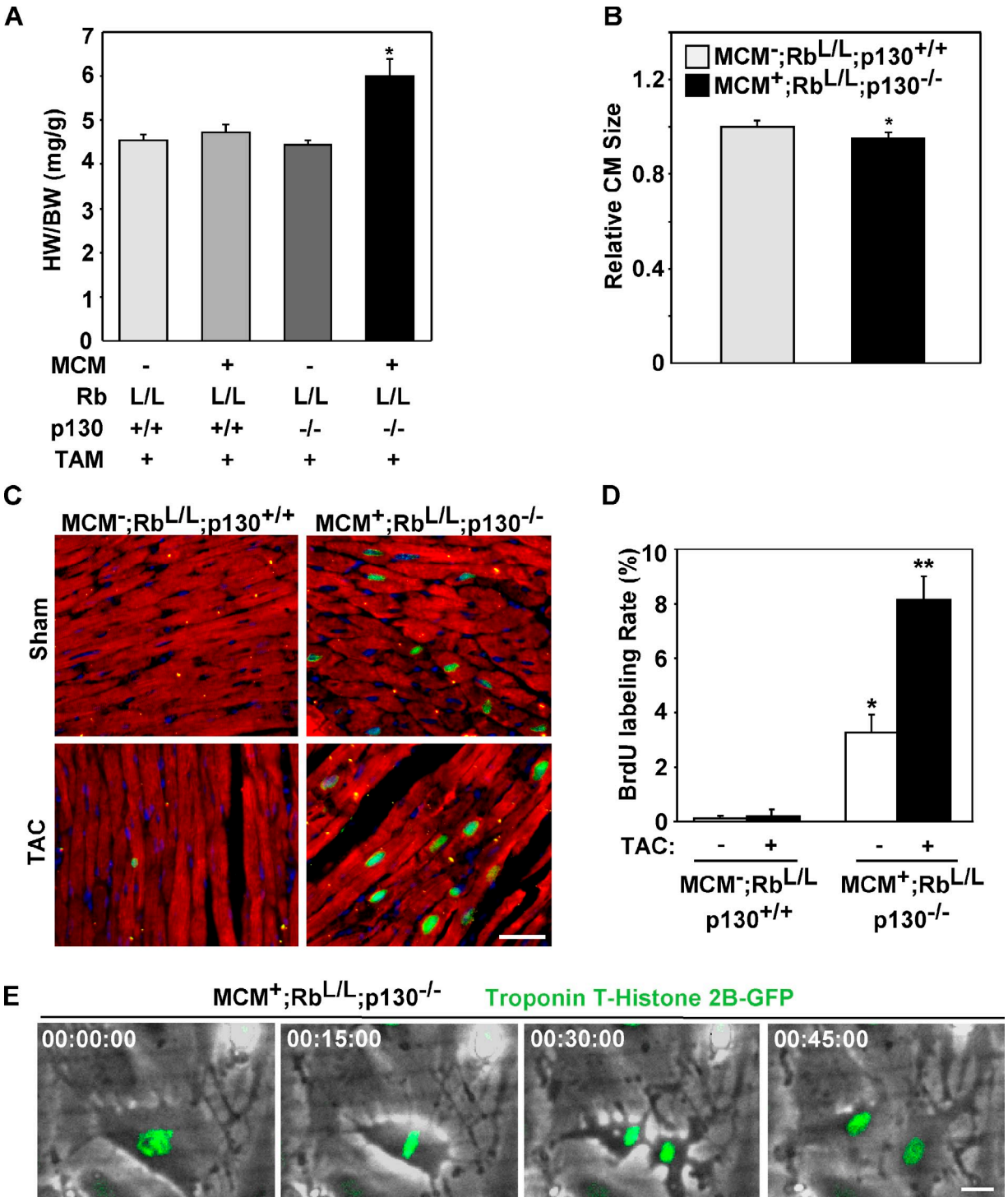

Figure 5. **IDKO ACMs spontaneously proliferate.** (A) IDKO hearts displayed a 32% increase in heart weight to body weight ratio (HW/BW; $n = 4$ per group; *, $P < 0.01$). (B) Relative cell size of IDKO ACMs was 5% smaller than control ACM ($n = 4$ per group; *, $P < 0.05$). CM, cardiac myocyte. (C) Immunofluorescence images of myocardial sections showing that IDKO ACMs reenter S phase in vivo (green, BrdU; red, troponin C; blue, DAPI). Bar, 40 µm. (D) Quantitation of BrdU labeling ($n = 3$ per group). *, $P = 0.003$ for sham-operated IDKO versus control; **, $P < 0.0001$ for TAC-operated IDKO versus control. (A, B, and D) Error bars represent the SEM. (E) IDKO cardiac myocytes complete cytokinesis in vitro. Histone 2B–GFP was expressed under control of the troponin T promoter (green) to visualize cardiomyocyte nuclei. The images were collected for 24 h at 15-min intervals (see Video 1). Bar, 15 µm.

Interestingly, HP1-γ is not present at the Myc promoter, which is up-regulated in ACMs in response to hypertrophic signals. Normal cellular localization of HP1 was disrupted in IDKO cardiac myocytes (Fig. 7 D).

Rb/p130 is dispensable for Suv39h1-mediated H3K9me3

The fact that IDKO cardiac myocytes demonstrated persistent H3K9me3 at E2F-dependent promoters suggested that Rb/p130

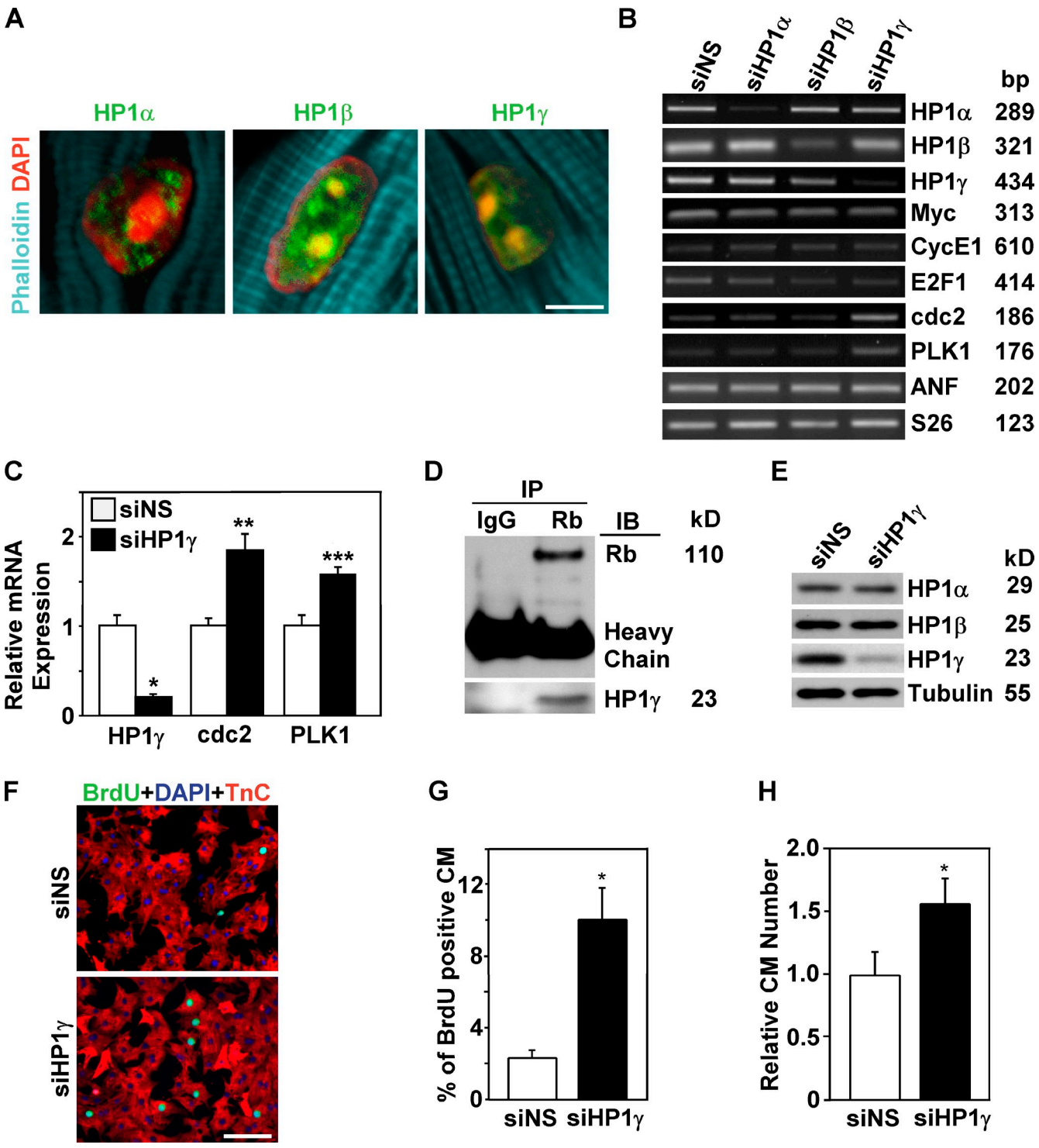

Figure 6. **HP1-γ is required for irreversible silencing of proliferation-associated genes in ACMs.** (A) HP1-α, -β, and -γ are expressed in ACMs. (B) Semi-quantitative RT-PCR shows that expression of cdc2 and PLK1 are increased when HP1-γ is depleted in ACMs with siRNA. si NS, NS siRNA. (C) Quantitation of data in B by real-time PCR. *, P = 0.002; **, P = 0.002; ***, P = 0.007. (D) IP assay demonstrates that Rb associates with HP1-γ in adult mice hearts. IB, immunoblotted. (E–H) NRVMs were transfected with NS or HP1-γ siRNA. After 48 h in serum-free media, cells were either collected for Western blot analysis (E) or stimulated with 20% FBS for 24 h in the presence of BrdU. (F) Cells were stained for BrdU and troponin C (TnC), and nuclei were counter-stained with DAPI. Bar, 100 µm. (G and H) The percentage of BrdU-positive nuclei (G; *, P = 0.002) as well as total cell number (H; *, P = 0.038) was increased in HP1-γ siRNA–transfected NRVMs. Error bars represent the SEM from three replicates.

deletion did not affect H3K9me3 methylation. Recent studies have suggested that, in contrast to earlier studies (Nielsen et al., 2001), Suv39h1-dependent methylation is Rb independent (Gonzalo et al., 2005; Siddiqui et al., 2007). To clarify the role of Suv39h1 on H3K9me3 levels in ACMs, siRNA was used to deplete Suv39h1 in control or IDKO cardiac myocytes. Transient transfection of Suv39h1 siRNA oligonucleotides into ACMs efficiently reduced expression of Suv39h1 (Fig. 8, A and B), which

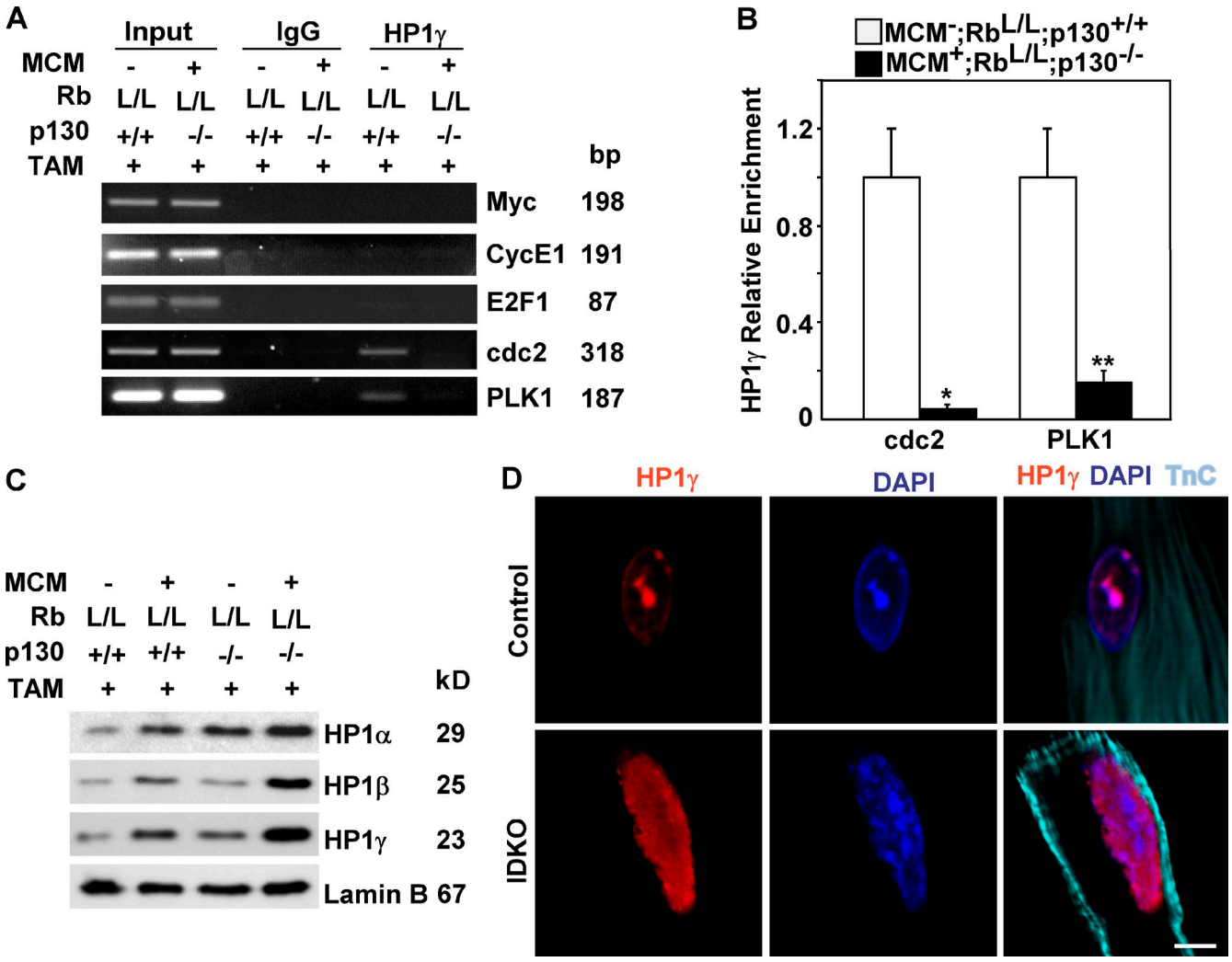

Figure 7. **Rb/p130-dependent recruitment of HP1-γ to E2F-responsive promoters is essential for irreversible silencing of proliferation-associated genes in ACMs.** (A) HP1-γ bound to G2/M and cytokinesis genes in an Rb/p130-dependent manner as shown by ChIP using chromatin extracts from purified ACMs. (B) Quantitation of HP1-γ enrichment at the indicated promoters by real-time PCR. Error bars represent the SEM from three replicates. *, P = 0.018; **, P = 0.003. (C) A Western blot showing HP1-α, -β, and -γ expression in ventricles from mice with the indicated genotypes. (D) HP1-γ colocalized with heterochromatin in control ACM. IDKO ACM lost heterochromatin, and HP1-γ staining is diffused. TnC, troponin C. Bar, 5 µm.

resulted in a comparable reduction of H3K9me3 in both genotypes. Knockdown of Suv39h1 had a similar effect on cell cycle gene expression as was seen in HP1-γ–deficient cells (Fig. 8 B). Cdc2 and PLK1 mRNA levels increased 1.5–2-fold ($P < 0.05$). The binding of HP1 to H3K9 is Suv39h1 dependent (Bannister et al., 2001; Lachner et al., 2001; Peters et al., 2001). Proliferation-associated genes were up-regulated either by depleting Suv39h1 or Rb/p130, suggesting that both are required for permanent gene silencing by HP1-γ (Fig. 8 C).

Discussion

It has been recognized for some time that many lower vertebrates have a robust capacity to regenerate organs, including the heart. This was felt to be lost in mammals, but a recent study has suggested that it is retained through embryonic and perinatal life (Porrello et al., 2011). However, it is clear that the adult mammalian heart has lost this regenerative capacity. If there is limited new cardiac myocyte formation, it arises from a nonmyocyte pool of progenitor cells (Davis et al., 2006; Bergmann et al., 2009). In the present study, we have investigated the molecular basis of this postmitotic state of ACM and demonstrated that heterochromatin accumulates in ACMs as they lose proliferative potential. We show that Rb and p130 are critical for targeting and maintaining a subset of E2F-dependent genes in heterochromatin in ACMs. Rb and p130 permanently silence these G2/M and cytokinesis genes via the recruitment of HP1-γ, an essential component of heterochromatin to the promoters of these genes. Reversing these epigenetic changes was also associated with reexpression of fetal cardiac genes, which we believe is analogous to the reexpression of Gata4 that was seen in dedifferentiated cardiac myocytes in zebrafish (Kikuchi et al., 2010). Left ventricular dysfunction was also seen, but whether this is a direct consequence of the epigenetic manipulations we made or is a secondary effect related to the dedifferentiation of IDKO ACMs will need to be determined; however, the contractile

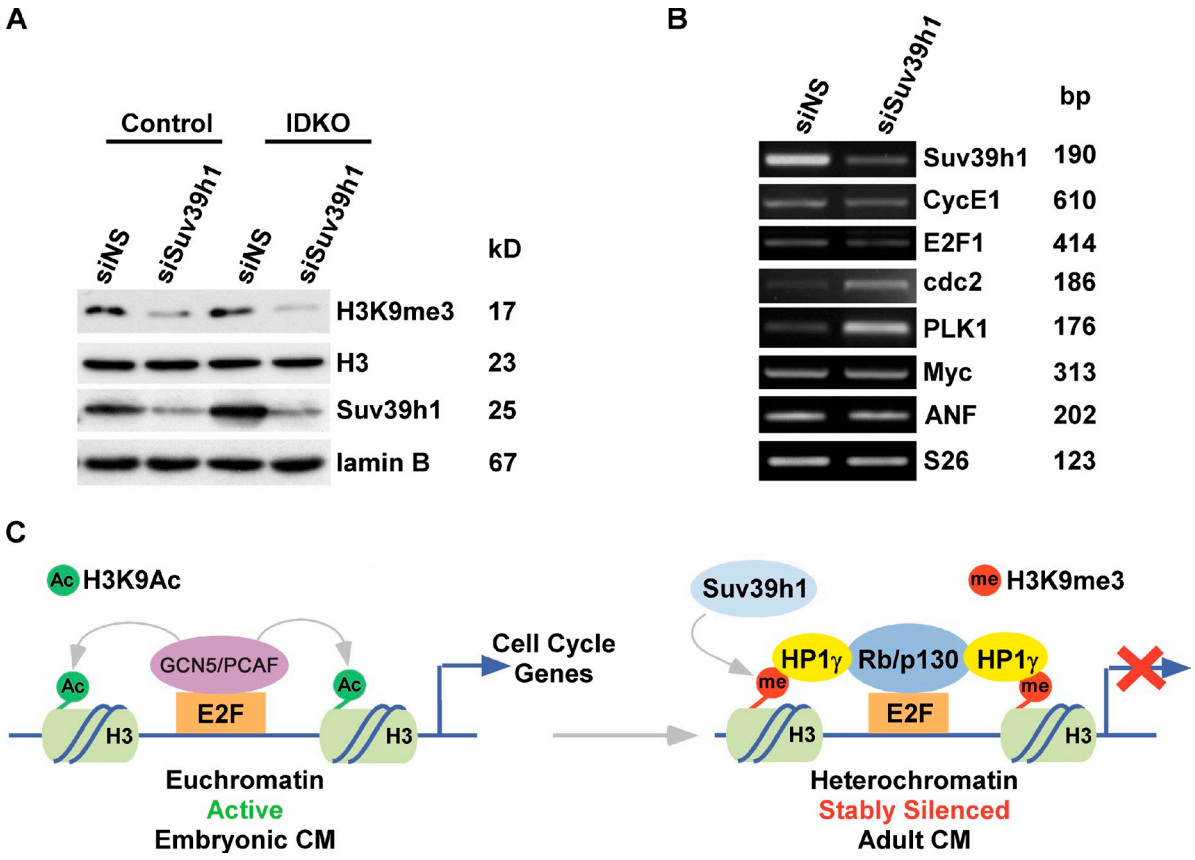

Figure 8. **Rb/p130 is dispensable for Suv39h1-mediated H3K9me3.** (A) Rb/p130 deletion did not affect methyltransferase activity of Suv39h1 on H3K9. Comparable reduction of H3K9me3 was detected after depletion of Suv39h1 by siRNA in ACMs isolated from control and IDKO mice hearts 4 wk after TAM treatment. siNS, NS siRNA. (B) Semiquantitative RT-PCR demonstrating increased expression of cdc2 and PLK1 after Suv39h1 is depleted in ACMs with siRNA. CBP, cAMP response element-binding–binding protein. (C) A schematic model depicting Rb/p130-dependent epigenetic modifications associated with cell cycle gene regulation in embryonic cardiac myocytes and ACMs and Rb/p130-dependent heterochromatin formation in ACMs based on our results and published data (Roth et al., 2001; Daniel et al., 2005; Grewal and Jia, 2007; Jin et al., 2011). CM, cardiac myocyte; PCAF, P300/cAMP response element-binding CBP–associated factor.

defect appears to be at the level of the myocyte (Fig. S3 D). Of note, heart regeneration in zebrafish, which occurs by cardiac myocyte dedifferentiation and proliferation, is well tolerated, so this contractile defect associated with epigenetic dedifferentiation in ACMs may underlie the reason why mammalian cardiac myocytes have evolved to be postmitotic (Jopling et al., 2010; Kikuchi et al., 2010).

Heterochromatin is a tightly packed and transcriptionally silent form of DNA, which comes in two varieties: constitutive and facultative. Constitutive heterochromatin is usually repetitive and cell type independent and occurs around the chromosome centromere and near telomeres. In contrast, facultative heterochromatin is an acquired form that is cell type specific and is the result of genes that are silenced through histone methylation (Oberdoerffer and Sinclair, 2007). Although heterochromatin formation has been reported in postmitotic skeletal myotubes, the effects of heterochromatin on the expression of proliferation-promoting genes were not determined (Brero et al., 2005). Heterochromatin has a characteristic histone modification profile, which is distinguished by hypoacetylation and enrichment of H3K9me3. Our study demonstrates that the chromatin of proliferating embryonic cardiac myocytes is hyperacetylated (H3K9/14, H3K18, and H3K27), but, after adult differentiation, acetylation decreases, and histone methylation associated with transcriptional repression (H3K9me3 and H3K27me3) predominates.

The relationship of H3K9me3 and heterochromatin is well established, and recent studies (Bannister et al., 2001; Dillon, 2004; Daniel et al., 2005; Grewal and Jia, 2007) have demonstrated that Suv39h1-mediated H3K9me3 and the binding of HP1 to H3K9me3 through its chromodomain are necessary for the assembly of facultative heterochromatin. Heterochromatin is a self-assembling framework of tethers (H3K9me3) and adaptors (HP1) where the HP1 molecules bound to different nucleosomes dimerize through their chromoshadow domains, leading to chromatin condensation (Grewal and Jia, 2007). Although depletion of Rb in p130-null ACMs disrupted heterochromatin formation globally (Fig. 4 C), there was no change in total or E2F-dependent, promoter-associated H3K9me3 or H3K27me3 levels. This implies that these histone modifications may be required but are not sufficient for maintaining heterochromatin in ACMs. Superficially, these results seem to differ from a previous study (Nielsen et al., 2001) in nonmyocytes in which Rb was required for H3K9 methylation of E2F-dependent promoters.

However, they are consistent with the conclusion that the recruitment of HP1 to H3K9 methylation is Rb/p130 dependent. We have explored this issue in ACMs and demonstrated that deleting Rb reduced H3K9me2 but had no effect on H3K9me3 levels (Fig. 4 B). Thus, whether the previous study was related to differences in the precise H3K9 methylation or was related to cell type–specific utilization or interaction of these factors will need to be determined. Regardless, our data suggest that H3K9me3 alone is not sufficient to recruit HP1 in ACMs, and additional factors such as Rb family members are required for efficient binding. The ability to reverse the postmitotic state was also shown in a recent study in which concomitant inactivation of p14ARF and Rb led to skeletal myotube cell cycle reentry, loss of differentiation properties, and up-regulation of cytokinetic machinery (Pajcini et al., 2010). Although these authors did not examine the epigenetic impact of these gene manipulations, our data would suggest that Rb may be the key to recruiting a multimeric chromatin-remodeling complex in postmitotic cells and explain why certain genes are specifically targeted for incorporation into heterochromatin. Irreversible growth arrest in myogenic differentiation requires the LXCXE-binding motif in Rb (Chen and Wang, 2000), indicating that at least one additional factor is necessary for Rb to induce terminal differentiation, as the LXCXE pocket is not required for Rb–E2F interactions. HP1 proteins contain an LXCXE (or LXCXD) motif (Williams and Grafi, 2000) and interact with both Rb and p130 (Panteleeva et al., 2007), and their recruitment to methylated H3K9 is Rb dependent (Nielsen et al., 2001).

HP1 belongs to a highly conserved family of chromatin proteins, with homologues that are found from fission yeast to mammals (Huisinga et al., 2006). The role of HP1 family members during differentiation has received limited investigation but appears to be complex and developmentally dependent (Zhang et al., 2002; Cammas et al., 2004; Feldman et al., 2006; Agarwal et al., 2007; Panteleeva et al., 2007; Yahi et al., 2008; Takanashi et al., 2009). HP1-α can negatively regulate differentiation by inhibiting tissue-specific factors at an early developmental stage (Zhang et al., 2002; Yahi et al., 2008) while promoting differentiation at later stages by mediating repression of cell cycle genes and cell cycle exit (Panteleeva et al., 2007). We have detected the expression of all three family members of HP1 in postmitotic cardiac myocytes; however, depletion of HP1-γ, but not HP1-α or HP1-β, resulted in reexpression of E2F-dependent genes in ACMs. HP1-γ is also present at the promoters of G2/M and cytokinesis genes in ACMs, and this binding is Rb and p130 dependent. Loss of HP1-γ recruitment appeared to be the key factor in the disruption of heterochromatin and the ability to reenter the cell cycle. Our results demonstrate that HP1-γ is specifically essential for stably repressing proliferation-promoting genes in ACMs and, although HP1 family members share similar structure (HP1-α and HP1-β), could not compensate for the loss of function of HP1-γ in cardiac myocytes. This result demonstrates that HP1 proteins, in contrast to Rb family members, are not functionally redundant. Why HP1-γ was specifically recruited to G2/M and cytokinesis genes in ACMs versus other E2F-dependent promoters is unclear. However, E2F binding specificity to target promoters is effected by numerous factors including nonconsensus genomic sequences and interactions of E2F with other factors that bind to the target promoters (Rabinovich et al., 2008). Binding of specific E2F family members and their interactions with other factors can differentially regulate subsets of E2F-dependent cell cycle genes (Caretti et al., 2003). Determining how particular HP1 family members are recruited to specific subsets of genes and their differential effects on transcription is a critical question.

ACMs also displayed higher levels of H3K27me3, the other repressive histone mark associated with heterochromatin, compared with embryonic cardiac myocytes. We chose to focus on the regulation of H3K9me3, Rb, and HP1-γ, given their well-established roles in permanent gene silencing and localization to heterochromatin. However, H3K27me3 can also be important for stable gene repression, including suppression of E2F-dependent genes, in certain contexts (Blais et al., 2007). Given that H3K27me3 is relatively enriched in ACM euchromatin, not heterochromatin, it will need to be determined what role, if any, it has in heterochromatin formation in ACMs and whether it contributes to the irreversible cell cycle exit seen in ACMs.

In summary, we have demonstrated that epigenetic modifications play a critical role in cardiac growth and differentiation. Actively proliferating embryonic cardiac myocytes enriched for H3K9/14Ac express high levels of proliferation-promoting genes. Terminally differentiated ACMs express high levels of Rb and p130, which serve as a bridge to link H3K9me3 and heterochromatin formation through their interaction with HP1-γ. Heterochromatin stably represses the expression of proliferation-promoting genes and maintains the postmitotic phenotype of ACMs (Fig. 8 C). The ability to restore ACMs' proliferative potential in vivo could lead to regenerative approaches similar to what occurs naturally in zebrafish hearts (Jopling et al., 2010; Kikuchi et al., 2010). These findings have important implications for promoting regeneration of the injured mammalian hearts and suggest that epigenetic manipulation of cardiac myocytes may be a viable therapeutic approach.

Materials and methods

Animal studies

$CRb^{L/L};p130^{-/-}$ mice have been previously described (MacLellan et al., 2005). To create inducible, cardiac-specific Rb- and p130-null mice, $Rb^{L/L};p130^{-/-}$ mice were bred to α-MHC–MCM mice, resulting in $MCM;Rb^{L/L};p130^{+/-}$ mice. Rb was deleted in ACMs after the Cre activation by TAM (Zhong et al., 2006). 8-wk-old mice carrying MCM were fed with TAM-containing chow (400 mg TAM citrate/kg supplemented standard diet Global 2016 pellets; Harlan Teklad Europe) for 14 d. Experiments were performed 4 wk after stopping TAM treatment unless specifically indicated. For TAC, a fixed pressure overload was obtained by surgically constricting the transverse aorta as previously described (Xiao et al., 2001). In brief, adult mice weighing 20–25 g were anesthetized by an i.p. injection of 60 mg/kg sodium pentobarbital. Microsurgical procedures were performed under a dissecting microscope (PZM III; World Precision Instruments, Inc.). Endotracheal intubation was performed using a blunt 20-gauge needle that was then connected to a volume-cycled rodent ventilator (SAR-830/P; IITC Life Science) with a tidal volume of 0.2 ml and a respiratory rate of 120/min. The chest was entered in the second intercostal space at the top left aortic arch, the transverse aorta was isolated, and aortic constriction was performed by tying a 7–0 nylon suture ligature against a 20-guage needle. The needle was then removed to yield a constriction of 0.4 mm in diameter. All animals were handled and maintained in accordance with institutional guidelines and the National Institutes of Health Guide for the Care and Use of Laboratory Animals.

Isolation and analysis of cardiac myocytes

Isolation of ACMs was performed by collagenase/protease digestion as previously described (Mitra and Morad, 1985; Pott et al., 2005). 9–13-wk-old mice were i.p. injected with heparin (2,000 U/mouse). 20 min after heparin injection, the heart was removed from the chest, cannulated via the ascending aorta, and mounted on a Langendorff perfusion apparatus. The heart was perfused for 4 min with myocyte buffer at 37°C. Then, the perfusion was switched to an enzyme solution containing 1.0 mg/ml collagenase type 2 (Worthington Biochemical Corp.), 0.1 mg/ml protease XIV (Sigma-Aldrich), and 0.015 mg/ml DNase I grade 2 (Roche). After 2 min of perfusion, the enzyme solution was supplemented with 40 µl of 100 mM $CaCl_2$, and perfusion was continued for another 8 min. After atria and aorta were removed, the ventricles were cut into two pieces and disaggregated with forceps (No. 5/45; Dumont) in 5 ml enzyme solution. The resulting tissue cell suspension was transferred to a 15-ml conical tube and incubated for 3–5 min to allow for further digestion. Digestion was stopped by adding 5 ml of stopping buffer (myocyte buffer plus 2.5% BSA and 0.1 mM $CaCl_2$). After isolation, the dissociated cells were collected in modified Tyrode's solution containing the following (in mmol/liter): 136 NaCl, 5.4 KCl, 10 Hepes, 1.0 $MgCl_2$, 0.33 NaH_2PO_4, 0.2 $CaCl_2$, 10 dextrose, and 10 2,3-butanedione monoxime, pH 7.4, with NaOH. The cells were pelleted at 18 *g* for 2 min, resuspended in plating medium, and plated on 10 µg/ml Laminin-coated flasks (Invitrogen) or chamber slides to allow attachment. After 2 h, serum-containing plating media were switched to culture media (Kabaeva et al., 2008). The culture media were prepared by supplementing MEM (Invitrogen) with 1% penicillin-streptomycin-glutamine (PSG; Invitrogen), 1% insulin-transferrin-selenium (ITS; Sigma-Aldrich), 4 mM $NaHCO_3$, 10 mM Hepes, 0.2% BSA, and 25 µM blebbistatin (Toronto Research Chemicals). Culture media were changed every day. Plating media were supplemented with 5% FBS (Invitrogen). To measure ACM size, the phase-contrast images of isolated ACM were acquired using a microscope (Axiovert 200; Carl Zeiss), and cell size was calculated using ImageJ (National Institutes of Health). 100 ACMs per heart were examined for cell size. Fetal mouse ventricular myocytes and NRVMs were isolated as previously described (Ueno et al., 1988). Fetal mouse cardiac myocytes were prepared from ventricles of E15.5 mice embryos, and NRVMs were prepared from the ventricles of 2-d-old Sprague-Dawley rats. In brief, cells were isolated by four cycles of enzymatic digestion with gentle mechanical disaggregation. Cells were dissociated at 37°C and 40 rpm in Ca^{2+}- and Mg^{2+}-free PBS supplemented with 0.1% trypsin, 0.1% collagenase, and 0.025% DNAase (Worthington Biochemical Corp.). After the final cycle of digestion, the dissociated cells were pooled and purified by density centrifugation through a discontinuous Percoll gradient (GE Healthcare). Cells were then resuspended in culture medium (DME: M199 = 4:1, 1% PSG, and 1% ITS) containing 10% neonatal calf serum (Invitrogen) and plated on polystyrene culture dishes treated with 0.1% gelatin (ICN Biochemicals, Inc.). After 12–16 h, NRVMs were maintained in culture in serum-free medium.

Histological analysis and BrdU studies

For histology, hearts were fixed overnight in 10% buffered formalin and then routinely processed. To quantify DNA synthesis, sham or TAC was performed 1 wk after TAM treatment. 5 d after surgery, mice were injected with 50 mg/kg BrdU every 12 h for 2 d. The animals were euthanized, and their hearts were recovered 4 h after the last injection. For in vitro studies, NRVMs were transfected with HP1-γ siRNA or negative control siRNA. After a further 48 h in serum-free media, cultures were stimulated with 20% FBS in the presence of 10 µm BrdU labeling reagent. Then, cells were fixed and subjected to immunostaining.

Protein analyses

Heart tissue, isolated embryonic cardiac myocytes, or ACMs were used to obtain nuclear extracts. Heart tissues were homogenized in homogenization buffer (250 mM sucrose, 10 mM Tris, pH 7.4, 1 mM EDTA, 0.5% NP-40, 1 mM Na_3VO_4, 1 mM NaF, and protease inhibitor cocktail). Isolated cardiac myocytes were resuspended in homogenization buffer and centrifuged at 1,000 *g* for 10 min at 4°C. Pellets were resuspended in 0.3 ml homogenization buffer, layered on 1 M sucrose, and recentrifuged at 1,600 *g* for 5 min at 4°C. The nuclear protein was extracted with sonication in EBC250 buffer (25 mM Tris-HCl, pH 8.0, 250 mM NaCl, 1 mM NaF, 1 mM Na_3VO_4, 0.5% NP-40, and protease inhibitor). Equal amounts of nuclear protein (5–50 µg) were separated on SDS-PAGE gels, transferred to polyvinylidene fluoride membrane, and hybridized using an appropriate primary antibody and HRP-conjugated secondary antibody for subsequent detection by ECL. For IP, 1 mg nuclear extract from an adult mouse heart was incubated with 5 µg anti-Rb (G3-245; BD) at 4°C overnight, and precipitates were subjected to Western blot analysis.

Antibodies to Rb (G3-245; BD), p130 (C-20; Santa Cruz Biotechnology, Inc.), H3K9/14Ac (06-599; Millipore), H3K27Ac (07–360; Millipore), H3K9me2 (ab7312; Abcam), H3K9me3 (ab8898; Abcam), H3K27me3 (07–449; Millipore), phosphor-Histone (Ser10, 04–817; Millipore), Ezh1 (ab64850; Abcam), Ezh2 (39639; Active Motif), G9a (ab31874; Abcam), Suv39h1 (MG44; Millipore), HP1-γ (MAB3450; Millipore), phosphor-Histone (Ser10; Millipore), BrdU (ab6326; Abcam), tubulin (T8660; Sigma-Aldrich), Laminin B (Santa Cruz Biotechnology, Inc.), and H3 (05–928; Millipore) were purchased commercially. Anti-H3K18Ac and -p107 were provided by S.K. Kurdistani (University of California, Los Angeles, Los Angeles, CA).

Immunostaining and confocal analysis

Isolated cardiac myocyte cells were fixed with 4% PFA. Paraffin-embedded tissue sections or fixed cells were immunostained following standard protocols. Antibodies to BrdU (ab6326), HP1-α (15.19s2; Millipore), HP1-β (MAB3448; Millipore), HP1-γ (MAB3450), troponin C (E-7; Santa Cruz Biotechnology, Inc.), troponin I (H-170; Santa Cruz Biotechnology, Inc.), and sarcomeric MHCs (MF20; Developmental Studies Hybridoma Bank) were purchased commercially. Phalloidin and secondary antibodies were purchased from Invitrogen.

Nuclei were visualized by DAPI staining. For calculation of heterochromatin percentages, >100 nuclei per heart were examined by two independent blinded observers. Images were acquired with a microscope (Axiovert 200) equipped with imaging software (AxioVision 4.6; Carl Zeiss) at room temperature. A charge-coupled device camera (CoolSnap fx; Photometrics) was used for immunofluorescence staining, and a microscopy camera (AxioCam MRc; Carl Zeiss) was used for immunohistochemistry or immunocytochemistry staining. For confocal analysis, images were acquired with a true confocal scanner laser-scanning microscope system (SP2 AOBS; Leica) with 40× 1.3 NA and 63× 1.4 NA oil immersion objectives at room temperature. All images within the same panel were processed similarly using Photoshop (version 6.0; Adobe).

siRNA and RNA analysis

ACMs were transfected with 50 nM HP1-γ siRNA or negative control siRNA (QIAGEN) by using Lipofectamine RNAiMAX (QIAGEN). 24 h after transfection, cells were stimulated with 20% FBS for 24 h. For RT-PCR, total RNA was isolated from cells or tissue using TRI Reagent (Sigma-Aldrich). First-strand cDNA was generated from 1 µg of total RNA by using a reverse transcription kit (Omniscript; QIAGEN). Real-time quantitative PCR was conducted using the ABI PRISM 7700 sequence detection system (Taqman; Applied Biosystems). PCR amplicons were detected by fluorescent detection of SYBR green (QuantiTect SYBR green PCR kit; QIAGEN). The siRNA oligonucleotide sequences used are as follows: HP1-α, 5′-GGCUUUUCUGAGGAGCACATT-3′ (sense) and 5′-UGUGCUCCUCAAGAAAAGCCTT-3′ (antisense); HP1-β, 5′-GGAAGCCAAUGUCAAGUGCTT-3′ (sense) and 5′-GCACUUGACAUUGGCUUCCTT-3′ (antisense); and HP1-γ, 5′-GCAGCGGAGAGUUAAUGUUTT-3′ (sense) and 5′-AACAUUAACUCUCCGCUGCTG-3′ (antisense). The Suv39h1 oligonucleotide sequences were previously published (Ait-Si-Ali et al., 2004). NS siRNA (QIAGEN) was used as a negative control.

ChIP

Isolated cardiac myocytes were fixed with 1% formaldehyde for 10 min at room temperature, and then 0.125 M glycine was added and incubated for 5 min at room temperature. To release the nuclei, cells were suspended in Mg-nonionic (NI)–NP-40 buffer (15 mM Tris-HCl, pH 7.5, 5 mM $MgCl_2$, 60 mM KCl, 0.5 mM DTT, 15 mM NaCl, 300 mM sucrose, and 1% NP-40) and incubated on ice for 20 min. Nuclei from the NP-40–lysed cells were spun down and washed in Ca-NI buffer (15 mM Tris-HCl, 1 mM $CaCl_2$, pH 7.5, 60 mM KCl, 0.5 mM DTT, 15 mM NaCl, and 300 mM sucrose). After they were spun down, pellets were resuspended in Ca-NI buffer containing 25 µg/ml *Staphylococcus aureus* nuclease (Roche) and incubated on ice for 30 min. After centrifugation at 3,500 rpm for 5 min at 4°C, cell pellets were lysed by sonication on ice with nuclear lysis buffer (50 mM Tris-Cl, pH 8.1, 10 mM EDTA, 1% SDS, and protease inhibitors). After centrifugation at 13,000 rpm for 10 min at 4°C, the lysates were diluted 10 times with dilution buffer (0.01% SDS, 1.1% Triton X-100, 1.2 mM EDTA, 16.7 mM Tris-Cl, pH 8.1, 167 mM NaCl, and protease inhibitor). After preclearing with 30 µl Protein A/G Dynabeads (Invitrogen), primary antibodies specific to H3K9me3 (Millipore), H3K27me3 (Millipore), and HP1-γ (MAB3450) were added and incubated overnight at 4°C.

Normal mouse or rabbit IgG was used as a control. After IP, 60 µl Protein A/G Dynabeads was added and incubated for 3 h. Precipitates were washed with dialysis buffer (2 mM EDTA and 50 mM Tris-Cl, pH 8.0) twice, IP wash buffer (100 mM Tris-Cl, pH 8.0, 500 mM LiCl, 1% NP-40, and 1% deoxycholic acid) four times, and Tris-EDTA buffer twice. The complexes were eluted with 1% SDS and 0.1 M $NaHCO_3$. The eluates were incubated overnight at 65°C to reverse the formaldehyde cross-linking. After proteinase K treatment, DNA was extracted by phenol/chloroform/isoamyl alcohol and precipitated by ethanol. PCR was performed using Platinum Taq polymerase (Invitrogen). The primers used are as follows: cdc2, 5′-GGTAAAGCTCCCGGGATCCGCCAAT-3′ (sense) and 5′-GTGGACTGTCACTTTGGTGGCTGGC-3′ (antisense); cyclin E1, 5′-ACGCCCGTAAAAGAACACGCCC-3′ (sense) and 5′-CCGGCTTCGAGCGGGACATTTA-3′ (antisense); E2F1, 5′-AATGGAGGAGGCGTTCG-3′ (sense) and 5′-CCGCTGCCTGCAAAGT-3′ (antisense); PLK, 5′-AGTTTCAGTTCTAGAAGGCCGGGT-3′ (sense) and 5′-ATTGCCTGGGAAACCAGGAACGAA-3′ (antisense); and Myc, 5′-AAACTTTGCCCATTGCAGCG-3′ (sense) and 5′-GTTTCCAACGCCCAAAGGAA-3′ (antisense).

Real-time quantitative PCR

Real-time quantitative PCR was conducted using the ABI PRISM 7700 sequence detection system. PCR amplicons were detected by fluorescent detection of SYBR green (QuantiTect SYBR green PCR kit). Error bars represent the SEM from three replicates.

TLVM

Freshly isolated ACMs were initially cultured in M199 medium supplemented with 5 mM creatine, 5 mM taurine, 2 mM L-carnitine, 1% PSG, 8% FBS, 25 µM blebbistatin, and 10 µM cytosine β-D-arabinofuranoside. After 48 h, blebbistatin was removed. After another 3 d, cytosine β-D-arabinofuranoside was removed. Cells were infected with an adenovirus expressing a fusion construct of histone 2B–GFP under control of the chicken troponin T promoter (Ad–chicken troponin T–H2B-GFP; provided by F. del Monte, Beth Israel Deaconess Medical Center, Boston, MA) on day 7. 2 d after infection, TLVM was performed using an inverted microscope equipped with a phase-contrast temperature-controlled motorized stage (DMIRE2; Leica). The 12.5-cm^2 flask with an air-permeable cap was maintained on the stage at 37°C in 95% air/5% CO_2 saturated with water, similar conditions to a regular CO_2 incubator. The bright-field and spin disc laser confocal images of cardiomyocyte cells were acquired at 37°C using a charge-coupled device camera (Hamamatsu Photonics) at 200× magnification using Volocity software (PerkinElmer) and collected at 15-min intervals.

Patch-clamp methods

ACMs were patch clamped in the whole-cell configuration of the patch-clamp technique in the current clamp mode (Xie et al., 2009). Patch pipettes (2–4-MΩ resistance) were filled with internal solution containing (mM) 110 K-aspartate, 30 KCl, 5 NaCl, 10 Hepes, 0.1 EGTA, 5 MgATP, 5 creatine phosphate, and 0.1 cAMP, pH 7.2, adjusted with KOH. Myocytes were superfused with standard Tyrode's solution containing (mM) 136 NaCl, 5.4 KCl, 0.33 Na_2PO_4, 1.8 $CaCl_2$, 1 $MgCl_2$, 10 glucose, and 10 Hepes, pH 7.4, adjusted with NaOH. All chemicals and reagents were purchased from Sigma-Aldrich. To induce ACM contraction, action potentials were elicited with trains of 20 square pulses (for 2 ms at 2–4 nA) at 300-, 500-, or 1,000-ms pacing cycle lengths. Voltage signals were monitored with a patch-clamp amplifier (Axopatch 200A; Molecular Devices) controlled by a personal computer using an acquisition board (Digidata 1200; Molecular Devices) driven by pCLAMP software (version 9.0; Molecular Devices). All experiments were performed at 37°C.

ACM contraction analysis

Patch-clamped ACMs were simultaneously imaged during pacing using a high-speed charge-coupled device–based camera (128 × 128 pixels; Cascade 128+; Photometrics) at ∼290 frames per second. The acquired video image data were then processed using Imaging Workbench software (version 6.0; INDEC BioSystems). ACM lengths were measured and analyzed using ImageJ software, and the percentage of change in myocyte length was calculated as a percentage for one minus the ratio of myocyte length at peak contraction over the length at rest. Contraction lengths were averaged over the 20 contractions evoked by the stimulus train for each myocyte.

Statistical analysis

All data are presented as the mean ± SEM. Results were compared by analysis of variance and Fisher's protected least significant difference tests with a significance of $P < 0.05$.

Online supplemental material

Fig. S1 shows heterochromatin formation in ACMs and is related to Fig. 1. Fig. S2 shows that cardiac myocytes from adult $MCM^{-};Rb^{L/L};p130^{+/+}$, $MCM^{+};Rb^{L/L};p130^{+/+}$, $MCM^{-};Rb^{L/L};p130^{-/-}$, and $MCM^{+};Rb^{L/L};p130^{-/-}$ mice differentiate normally before TAM treatment and is related to Fig. 3. Fig. S3 shows characterization of IDKO cardiac myocytes and is related to Fig. 3. Fig. S4 shows that proliferation-promoting gene expressions were up-regulated after depletion of Rb and p130 in ACMs; however, levels of H3K9me3 and H3K27me3 were unchanged. Fig. S4 shows up-regulation of proliferation-promoting gene expression after depletion of Rb and p130 in ACMs and is related to Fig. 4. Fig. S5 shows characterization of cardiac growth in IDKO hearts and is related to Fig. 5. Video 1 shows that Rb- and p130-null ACMs complete cytokinesis in vitro and is related to Fig. 5. Online supplemental material is available at http://www.jcb.org/cgi/content/full/jcb.201012049/DC1.

We would like to thank Nicole Petrochuk, Rui Zhang, and Roberto Ferrari for technical assistance and Michael Schneider for helpful discussion and reading of the manuscript. We are grateful to Dr. Siavash K. Kurdistani for antibodies and Dr. Federica del Monte for Ad–chicken troponin T–H2B-GFP.

This work was supported by National Institutes of Health (NIH) grants (HL70748 and HL080111) and Laubisch and Cardiovascular Development funds to W.R. MacLellan and Larry Hillblom Foundation (2007-D-003-NET) and NIH (DK077967) grants to P.C. Butler. Confocal laser-scanning microscopy was performed at the California NanoSystems Institute Advanced Light Microscopy/Spectroscopy shared resource facility at the University of California, Los Angeles, and was supported with funding from NIH–National Center for Research Resources shared resources (CJX1-443835-WS-29646) and National Science Foundation Major Research Instrumentation (CHE-0722519) grants.

Submitted: 8 December 2010
Accepted: 11 July 2011

References

Agarwal, N., T. Hardt, A. Brero, D. Nowak, U. Rothbauer, A. Becker, H. Leonhardt, and M.C. Cardoso. 2007. MeCP2 interacts with HP1 and modulates its heterochromatin association during myogenic differentiation. *Nucleic Acids Res.* 35:5402–5408. doi:10.1093/nar/gkm599

Ait-Si-Ali, S., V. Guasconi, L. Fritsch, H. Yahi, R. Sekhri, I. Naguibneva, P. Robin, F. Cabon, A. Polesskaya, and A. Harel-Bellan. 2004. A Suv39h-dependent mechanism for silencing S-phase genes in differentiating but not in cycling cells. *EMBO J.* 23:605–615. doi:10.1038/sj.emboj.7600074

Auth, T., E. Kunkel, and F. Grummt. 2006. Interaction between HP1alpha and replication proteins in mammalian cells. *Exp. Cell Res.* 312:3349–3359. doi:10.1016/j.yexcr.2006.07.014

Bannister, A.J., P. Zegerman, J.F. Partridge, E.A. Miska, J.O. Thomas, R.C. Allshire, and T. Kouzarides. 2001. Selective recognition of methylated lysine 9 on histone H3 by the HP1 chromo domain. *Nature*. 410:120–124. doi:10.1038/35065138

Bergmann, O., R.D. Bhardwaj, S. Bernard, S. Zdunek, F. Barnabé-Heider, S. Walsh, J. Zupicich, K. Alkass, B.A. Buchholz, H. Druid, et al. 2009. Evidence for cardiomyocyte renewal in humans. *Science*. 324:98–102. doi:10.1126/science.1164680

Bersell, K., S. Arab, B. Haring, and B. Kühn. 2009. Neuregulin1/ErbB4 signaling induces cardiomyocyte proliferation and repair of heart injury. *Cell*. 138:257–270. doi:10.1016/j.cell.2009.04.060

Blais, A., C.J. van Oevelen, R. Margueron, D. Acosta-Alvear, and B.D. Dynlacht. 2007. Retinoblastoma tumor suppressor protein–dependent methylation of histone H3 lysine 27 is associated with irreversible cell cycle exit. *J. Cell Biol.* 179:1399–1412. doi:10.1083/jcb.200705051

Brenner, C., and F. Fuks. 2007. A methylation rendezvous: reader meets writers. *Dev. Cell*. 12:843–844. doi:10.1016/j.devcel.2007.05.011

Brero, A., H.P. Easwaran, D. Nowak, I. Grunewald, T. Cremer, H. Leonhardt, and M.C. Cardoso. 2005. Methyl CpG–binding proteins induce large-scale chromatin reorganization during terminal differentiation. *J. Cell Biol.* 169:733–743. doi:10.1083/jcb.200502062

Camarda, G., F. Siepi, D. Pajalunga, C. Bernardini, R. Rossi, A. Montecucco, E. Meccia, and M. Crescenzi. 2004. A pRb-independent mechanism preserves the postmitotic state in terminally differentiated skeletal muscle cells. *J. Cell Biol.* 167:417–423. doi:10.1083/jcb.200408164

Cammas, F., M. Herzog, T. Lerouge, P. Chambon, and R. Losson. 2004. Association of the transcriptional corepressor TIF1beta with heterochromatin protein 1 (HP1): an essential role for progression through differentiation. *Genes Dev.* 18:2147–2160. doi:10.1101/gad.302904

Caretti, G., V. Salsi, C. Vecchi, C. Imbriano, and R. Mantovani. 2003. Dynamic recruitment of NF-Y and histone acetyltransferases on cell-cycle promoters. *J. Biol. Chem.* 278:30435–30440. doi:10.1074/jbc.M304606200

Chen, T.T., and J.Y. Wang. 2000. Establishment of irreversible growth arrest in myogenic differentiation requires the RB LXCXE-binding function. *Mol. Cell. Biol.* 20:5571–5580. doi:10.1128/MCB.20.15.5571-5580.2000

Chin, H.G., P.O. Estève, M. Pradhan, J. Benner, D. Patnaik, M.F. Carey, and S. Pradhan. 2007. Automethylation of G9a and its implication in wider substrate specificity and HP1 binding. *Nucleic Acids Res.* 35:7313–7323. doi:10.1093/nar/gkm726

Dahiya, A., S. Wong, S. Gonzalo, M. Gavin, and D.C. Dean. 2001. Linking the Rb and polycomb pathways. *Mol. Cell*. 8:557–569. doi:10.1016/S1097-2765(01)00346-X

Daniel, J.A., M.G. Pray-Grant, and P.A. Grant. 2005. Effector proteins for methylated histones: an expanding family. *Cell Cycle*. 4:919–926. doi:10.4161/cc.4.7.1824

Davis, M.E., P.C. Hsieh, T. Takahashi, Q. Song, S. Zhang, R.D. Kamm, A.J. Grodzinsky, P. Anversa, and R.T. Lee. 2006. Local myocardial insulin-like growth factor 1 (IGF-1) delivery with biotinylated peptide nanofibers improves cell therapy for myocardial infarction. *Proc. Natl. Acad. Sci. USA*. 103:8155–8160. doi:10.1073/pnas.0602877103

Dillon, N. 2004. Heterochromatin structure and function. *Biol. Cell*. 96:631–637. doi:10.1016/j.biolcel.2004.06.003

Drenckhahn, J.D., Q.P. Schwarz, S. Gray, A. Laskowski, H. Kiriazis, Z. Ming, R.P. Harvey, X.J. Du, D.R. Thorburn, and T.C. Cox. 2008. Compensatory growth of healthy cardiac cells in the presence of diseased cells restores tissue homeostasis during heart development. *Dev. Cell*. 15:521–533. doi:10.1016/j.devcel.2008.09.005

Feldman, N., A. Gerson, J. Fang, E. Li, Y. Zhang, Y. Shinkai, H. Cedar, and Y. Bergman. 2006. G9a-mediated irreversible epigenetic inactivation of Oct-3/4 during early embryogenesis. *Nat. Cell Biol.* 8:188–194. doi:10.1038/ncb1353

Fischle, W., Y. Wang, and C.D. Allis. 2003a. Histone and chromatin cross-talk. *Curr. Opin. Cell Biol.* 15:172–183. doi:10.1016/S0955-0674(03)00013-9

Fischle, W., Y. Wang, S.A. Jacobs, Y. Kim, C.D. Allis, and S. Khorasanizadeh. 2003b. Molecular basis for the discrimination of repressive methyl-lysine marks in histone H3 by Polycomb and HP1 chromodomains. *Genes Dev.* 17:1870–1881. doi:10.1101/gad.1110503

Gonzalo, S., M. García-Cao, M.F. Fraga, G. Schotta, A.H. Peters, S.E. Cotter, R. Eguía, D.C. Dean, M. Esteller, T. Jenuwein, and M.A. Blasco. 2005. Role of the RB1 family in stabilizing histone methylation at constitutive heterochromatin. *Nat. Cell Biol.* 7:420–428. doi:10.1038/ncb1235

Grewal, S.I., and S. Jia. 2007. Heterochromatin revisited. *Nat. Rev. Genet.* 8:35–46. doi:10.1038/nrg2008

Haberland, M., R.L. Montgomery, and E.N. Olson. 2009. The many roles of histone deacetylases in development and physiology: implications for disease and therapy. *Nat. Rev. Genet.* 10:32–42. doi:10.1038/nrg2485

Hsieh, P.C., V.F. Segers, M.E. Davis, C. MacGillivray, J. Gannon, J.D. Molkentin, J. Robbins, and R.T. Lee. 2007. Evidence from a genetic fate-mapping study that stem cells refresh adult mammalian cardiomyocytes after injury. *Nat. Med.* 13:970–974. doi:10.1038/nm1618

Huh, M.S., M.H. Parker, A. Scimè, R. Parks, and M.A. Rudnicki. 2004. Rb is required for progression through myogenic differentiation but not maintenance of terminal differentiation. *J. Cell Biol.* 166:865–876. doi:10.1083/jcb.200403004

Huisinga, K.L., B. Brower-Toland, and S.C. Elgin. 2006. The contradictory definitions of heterochromatin: transcription and silencing. *Chromosoma*. 115:110–122. doi:10.1007/s00412-006-0052-x

James, T.C., and S.C. Elgin. 1986. Identification of a nonhistone chromosomal protein associated with heterochromatin in *Drosophila melanogaster* and its gene. *Mol. Cell. Biol.* 6:3862–3872.

Jin, Q., L.R. Yu, L. Wang, Z. Zhang, L.H. Kasper, J.E. Lee, C. Wang, P.K. Brindle, S.Y. Dent, and K. Ge. 2011. Distinct roles of GCN5/PCAF-mediated H3K9ac and CBP/p300-mediated H3K18/27ac in nuclear receptor transactivation. *EMBO J.* 30:249–262. doi:10.1038/emboj.2010.318

Jopling, C., E. Sleep, M. Raya, M. Martí, A. Raya, and J.C. Belmonte. 2010. Zebrafish heart regeneration occurs by cardiomyocyte dedifferentiation and proliferation. *Nature*. 464:606–609. doi:10.1038/nature08899

Kabaeva, Z., M. Zhao, and D.E. Michele. 2008. Blebbistatin extends culture life of adult mouse cardiac myocytes and allows efficient and stable transgene expression. *Am. J. Physiol. Heart Circ. Physiol.* 294:H1667–H1674. doi:10.1152/ajpheart.01144.2007

Kellum, R. 2003. HP1 complexes and heterochromatin assembly. *Curr. Top. Microbiol. Immunol.* 274:53–77. doi:10.1007/978-3-642-55747-7_3

Kikuchi, K., J.E. Holdway, A.A. Werdich, R.M. Anderson, Y. Fang, G.F. Egnaczyk, T. Evans, C.A. Macrae, D.Y. Stainier, and K.D. Poss. 2010. Primary contribution to zebrafish heart regeneration by gata4(+) cardiomyocytes. *Nature*. 464:601–605. doi:10.1038/nature08804

Koitabashi, N., D. Bedja, A.L. Zaiman, Y.M. Pinto, M. Zhang, K.L. Gabrielson, E. Takimoto, and D.A. Kass. 2009. Avoidance of transient cardiomyopathy in cardiomyocyte-targeted tamoxifen-induced MerCreMer gene deletion models. *Circ. Res.* 105:12–15. doi:10.1161/CIRCRESAHA.109.198416

Krauss, V. 2008. Glimpses of evolution: heterochromatic histone H3K9 methyltransferases left its marks behind. *Genetica*. 133:93–106. doi:10.1007/s10709-007-9184-z

Lachner, M., D. O'Carroll, S. Rea, K. Mechtler, and T. Jenuwein. 2001. Methylation of histone H3 lysine 9 creates a binding site for HP1 proteins. *Nature*. 410:116–120. doi:10.1038/35065132

Laible, G., A. Wolf, R. Dorn, G. Reuter, C. Nislow, A. Lebersorger, D. Popkin, L. Pillus, and T. Jenuwein. 1997. Mammalian homologues of the Polycomb-group gene Enhancer of zeste mediate gene silencing in *Drosophila* heterochromatin and at *S. cerevisiae* telomeres. *EMBO J.* 16:3219–3232. doi:10.1093/emboj/16.11.3219

Lang, S.E., S.B. McMahon, M.D. Cole, and P. Hearing. 2001. E2F transcriptional activation requires TRRAP and GCN5 cofactors. *J. Biol. Chem.* 276:32627–32634. doi:10.1074/jbc.M102067200

Lee, M.H., B.O. Williams, G. Mulligan, S. Mukai, R.T. Bronson, N. Dyson, E. Harlow, and T. Jacks. 1996. Targeted disruption of p107: functional overlap between p107 and Rb. *Genes Dev.* 10:1621–1632. doi:10.1101/gad.10.13.1621

Lehnertz, B., Y. Ueda, A.A. Derijck, U. Braunschweig, L. Perez-Burgos, S. Kubicek, T. Chen, E. Li, T. Jenuwein, and A.H. Peters. 2003. Suv39h-mediated histone H3 lysine 9 methylation directs DNA methylation to major satellite repeats at pericentric heterochromatin. *Curr. Biol.* 13:1192–1200. doi:10.1016/S0960-9822(03)00432-9

Li, F., X. Wang, J.M. Capasso, and A.M. Gerdes. 1996. Rapid transition of cardiac myocytes from hyperplasia to hypertrophy during postnatal development. *J. Mol. Cell. Cardiol.* 28:1737–1746. doi:10.1006/jmcc.1996.0163

Luo, R.X., A.A. Postigo, and D.C. Dean. 1998. Rb interacts with histone deacetylase to repress transcription. *Cell*. 92:463–473. doi:10.1016/S0092-8674(00)80940-X

MacLellan, W.R., A. Garcia, H. Oh, P. Frenkel, M.C. Jordan, K.P. Roos, and M.D. Schneider. 2005. Overlapping roles of pocket proteins in the myocardium are unmasked by germ line deletion of p130 plus heart-specific deletion of Rb. *Mol. Cell. Biol.* 25:2486–2497. doi:10.1128/MCB.25.6.2486-2497.2005

Magnaghi-Jaulin, L., R. Groisman, I. Naguibneva, P. Robin, S. Lorain, J.P. Le Villain, F. Troalen, D. Trouche, and A. Harel-Bellan. 1998. Retinoblastoma protein represses transcription by recruiting a histone deacetylase. *Nature*. 391:601–605. doi:10.1038/35410

Mantela, J., Z. Jiang, J. Ylikoski, B. Fritzsch, E. Zacksenhaus, and U. Pirvola. 2005. The retinoblastoma gene pathway regulates the postmitotic state of hair cells of the mouse inner ear. *Development*. 132:2377–2388. doi:10.1242/dev.01834

Margueron, R., G. Li, K. Sarma, A. Blais, J. Zavadil, C.L. Woodcock, B.D. Dynlacht, and D. Reinberg. 2008. Ezh1 and Ezh2 maintain repressive chromatin through different mechanisms. *Mol. Cell*. 32:503–518. doi:10.1016/j.molcel.2008.11.004

Marino, S., M. Vooijs, H. van Der Gulden, J. Jonkers, and A. Berns. 2000. Induction of medulloblastomas in p53-null mutant mice by somatic inactivation of Rb in the external granular layer cells of the cerebellum. *Genes Dev.* 14:994–1004.

Martin, C., and Y. Zhang. 2005. The diverse functions of histone lysine methylation. *Nat. Rev. Mol. Cell Biol.* 6:838–849. doi:10.1038/nrm1761

Min, J., Y. Zhang, and R.M. Xu. 2003. Structural basis for specific binding of Polycomb chromodomain to histone H3 methylated at Lys 27. *Genes Dev.* 17:1823–1828. doi:10.1101/gad.269603

Minc, E., Y. Allory, H.J. Worman, J.C. Courvalin, and B. Buendia. 1999. Localization and phosphorylation of HP1 proteins during the cell cycle in mammalian cells. *Chromosoma*. 108:220–234. doi:10.1007/s004120050372

Minc, E., Y. Allory, J.C. Courvalin, and B. Buendia. 2001. Immunolocalization of HP1 proteins in metaphasic mammalian chromosomes. *Methods Cell Sci.* 23:171–174. doi:10.1023/A:1013168323754

Mitra, R., and M. Morad. 1985. A uniform enzymatic method for dissociation of myocytes from hearts and stomachs of vertebrates. *Am. J. Physiol.* 249:H1056–H1060.

Narita, M., S. Nűnez, E. Heard, M. Narita, A.W. Lin, S.A. Hearn, D.L. Spector, G.J. Hannon, and S.W. Lowe. 2003. Rb-mediated heterochromatin formation and silencing of E2F target genes during cellular senescence. *Cell*. 113:703–716. doi:10.1016/S0092-8674(03)00401-X

Nielsen, S.J., R. Schneider, U.M. Bauer, A.J. Bannister, A. Morrison, D. O'Carroll, R. Firestein, M. Cleary, T. Jenuwein, R.E. Herrera, and T.

Kouzarides. 2001. Rb targets histone H3 methylation and HP1 to promoters. *Nature*. 412:561–565. doi:10.1038/35087620

Oberdoerffer, P., and D.A. Sinclair. 2007. The role of nuclear architecture in genomic instability and ageing. *Nat. Rev. Mol. Cell Biol.* 8:692–702. doi:10.1038/nrm2238

Pajcini, K.V., S.Y. Corbel, J. Sage, J.H. Pomerantz, and H.M. Blau. 2010. Transient inactivation of Rb and ARF yields regenerative cells from postmitotic mammalian muscle. *Cell Stem Cell*. 7:198–213. doi:10.1016/j.stem.2010.05.022

Panteleeva, I., S. Boutillier, V. See, D.G. Spiller, C. Rouaux, G. Almouzni, D. Bailly, C. Maison, H.C. Lai, J.P. Loeffler, and A.L. Boutillier. 2007. HP1alpha guides neuronal fate by timing E2F-targeted genes silencing during terminal differentiation. *EMBO J.* 26:3616–3628. doi:10.1038/sj.emboj.7601789

Pasumarthi, K.B., and L.J. Field. 2002. Cardiomyocyte cell cycle regulation. *Circ. Res.* 90:1044–1054. doi:10.1161/01.RES.0000020201.44772.67

Peters, A.H., D. O'Carroll, H. Scherthan, K. Mechtler, S. Sauer, C. Schöfer, K. Weipoltshammer, M. Pagani, M. Lachner, A. Kohlmaier, et al. 2001. Loss of the Suv39h histone methyltransferases impairs mammalian heterochromatin and genome stability. *Cell*. 107:323–337. doi:10.1016/S0092-8674(01)00542-6

Porrello, E.R., A.I. Mahmoud, E. Simpson, J.A. Hill, J.A. Richardson, E.N. Olson, and H.A. Sadek. 2011. Transient regenerative potential of the neonatal mouse heart. *Science*. 331:1078–1080. doi:10.1126/science.1200708

Poss, K.D., L.G. Wilson, and M.T. Keating. 2002. Heart regeneration in zebrafish. *Science*. 298:2188–2190. doi:10.1126/science.1077857

Pott, C., K.D. Philipson, and J.I. Goldhaber. 2005. Excitation-contraction coupling in Na+-Ca2+ exchanger knockout mice: reduced transsarcolemmal Ca2+ flux. *Circ. Res.* 97:1288–1295. doi:10.1161/01.RES.0000196563.84231.21

Rabinovich, A., V.X. Jin, R. Rabinovich, X. Xu, and P.J. Farnham. 2008. E2F in vivo binding specificity: comparison of consensus versus nonconsensus binding sites. *Genome Res.* 18:1763–1777. doi:10.1101/gr.080622.108

Rice, J.C., S.D. Briggs, B. Ueberheide, C.M. Barber, J. Shabanowitz, D.F. Hunt, Y. Shinkai, and C.D. Allis. 2003. Histone methyltransferases direct different degrees of methylation to define distinct chromatin domains. *Mol. Cell*. 12:1591–1598. doi:10.1016/S1097-2765(03)00479-9

Roth, S.Y., J.M. Denu, and C.D. Allis. 2001. Histone acetyltransferases. *Annu. Rev. Biochem.* 70:81–120. doi:10.1146/annurev.biochem.70.1.81

Schuettengruber, B., D. Chourrout, M. Vervoort, B. Leblanc, and G. Cavalli. 2007. Genome regulation by polycomb and trithorax proteins. *Cell*. 128:735–745. doi:10.1016/j.cell.2007.02.009

Shao, Z., F. Raible, R. Mollaaghababa, J.R. Guyon, C.T. Wu, W. Bender, and R.E. Kingston. 1999. Stabilization of chromatin structure by PRC1, a Polycomb complex. *Cell*. 98:37–46. doi:10.1016/S0092-8674(00)80604-2

Shen, X., Y. Liu, Y.J. Hsu, Y. Fujiwara, J. Kim, X. Mao, G.C. Yuan, and S.H. Orkin. 2008. EZH1 mediates methylation on histone H3 lysine 27 and complements EZH2 in maintaining stem cell identity and executing pluripotency. *Mol. Cell*. 32:491–502. doi:10.1016/j.molcel.2008.10.016

Shi, Y. 2007. Histone lysine demethylases: emerging roles in development, physiology and disease. *Nat. Rev. Genet.* 8:829–833. doi:10.1038/nrg2218

Shogren-Knaak, M., H. Ishii, J.M. Sun, M.J. Pazin, J.R. Davie, and C.L. Peterson. 2006. Histone H4-K16 acetylation controls chromatin structure and protein interactions. *Science*. 311:844–847. doi:10.1126/science.1124000

Siddiqui, H., S.R. Fox, R.W. Gunawardena, and E.S. Knudsen. 2007. Loss of RB compromises specific heterochromatin modifications and modulates HP1alpha dynamics. *J. Cell. Physiol.* 211:131–137. doi:10.1002/jcp.20913

Soonpaa, M.H., and L.J. Field. 1994. Assessment of cardiomyocyte DNA synthesis during hypertrophy in adult mice. *Am. J. Physiol.* 266:H1439–H1445.

Takanashi, M., K. Oikawa, K. Fujita, M. Kudo, M. Kinoshita, and M. Kuroda. 2009. Heterochromatin protein 1gamma epigenetically regulates cell differentiation and exhibits potential as a therapeutic target for various types of cancers. *Am. J. Pathol.* 174:309–316. doi:10.2353/ajpath.2009.080148

Ueno, H., M.B. Perryman, R. Roberts, and M.D. Schneider. 1988. Differentiation of cardiac myocytes after mitogen withdrawal exhibits three sequential states of the ventricular growth response. *J. Cell Biol.* 107:1911–1918. doi:10.1083/jcb.107.5.1911

Walsh, S., A. Pontén, B.K. Fleischmann, and S. Jovinge. 2010. Cardiomyocyte cell cycle control and growth estimation in vivo—an analysis based on cardiomyocyte nuclei. *Cardiovasc. Res.* 86:365–373. doi:10.1093/cvr/cvq005

Wang, H., B. Larris, T.H. Peiris, L. Zhang, J. Le Lay, Y. Gao, and L.E. Greenbaum. 2007. C/EBPbeta activates E2F-regulated genes in vivo via recruitment of the coactivator CREB-binding protein/P300. *J. Biol. Chem.* 282:24679–24688. doi:10.1074/jbc.M705066200

Williams, L., and G. Grafi. 2000. The retinoblastoma protein - a bridge to heterochromatin. *Trends Plant Sci.* 5:239–240. doi:10.1016/S1360-1385(00)01653-8

Xiao, G., S. Mao, G. Baumgarten, J. Serrano, M.C. Jordan, K.P. Roos, M.C. Fishbein, and W.R. MacLellan. 2001. Inducible activation of c-Myc in adult myocardium in vivo provokes cardiac myocyte hypertrophy and reactivation of DNA synthesis. *Circ. Res.* 89:1122–1129. doi:10.1161/hh2401.100742

Xie, L.H., F. Chen, H.S. Karagueuzian, and J.N. Weiss. 2009. Oxidative-stress-induced afterdepolarizations and calmodulin kinase II signaling. *Circ. Res.* 104:79–86. doi:10.1161/CIRCRESAHA.108.183475

Yahi, H., L. Fritsch, O. Philipot, V. Guasconi, M. Souidi, P. Robin, A. Polesskaya, R. Losson, A. Harel-Bellan, and S. Ait-Si-Ali. 2008. Differential cooperation between heterochromatin protein HP1 isoforms and MyoD in myoblasts. *J. Biol. Chem.* 283:23692–23700. doi:10.1074/jbc.M802647200

Zhang, C.L., T.A. McKinsey, and E.N. Olson. 2002. Association of class II histone deacetylases with heterochromatin protein 1: potential role for histone methylation in control of muscle differentiation. *Mol. Cell. Biol.* 22:7302–7312. doi:10.1128/MCB.22.20.7302-7312.2002

Zhong, W., S. Mao, S. Tobis, E. Angelis, M.C. Jordan, K.P. Roos, M.C. Fishbein, I.M. de Alborán, and W.R. MacLellan. 2006. Hypertrophic growth in cardiac myocytes is mediated by Myc through a Cyclin D2-dependent pathway. *EMBO J.* 25:3869–3879. doi:10.1038/sj.emboj.7601252